COMSAT Laboratories

CR-159871

# FINAL REPORT

# THIN n-i-p RADIATION-RESISTANT SOLAR CELL FEASIBILITY STUDY

by

J. F. ALLISON, R. A. ARNDT, A. MEULENBERG, JR.
COMSAT Laboratories

Prepared for

NATIONAL AERONAUTICS AND SPACE ADMINISTRATION
Lewis Research Center
Contract NAS3-21280



COMMUNICATIONS SATELLITE CORPORATION
COMSAT Laboratories, Clarksburg, Maryland 20734

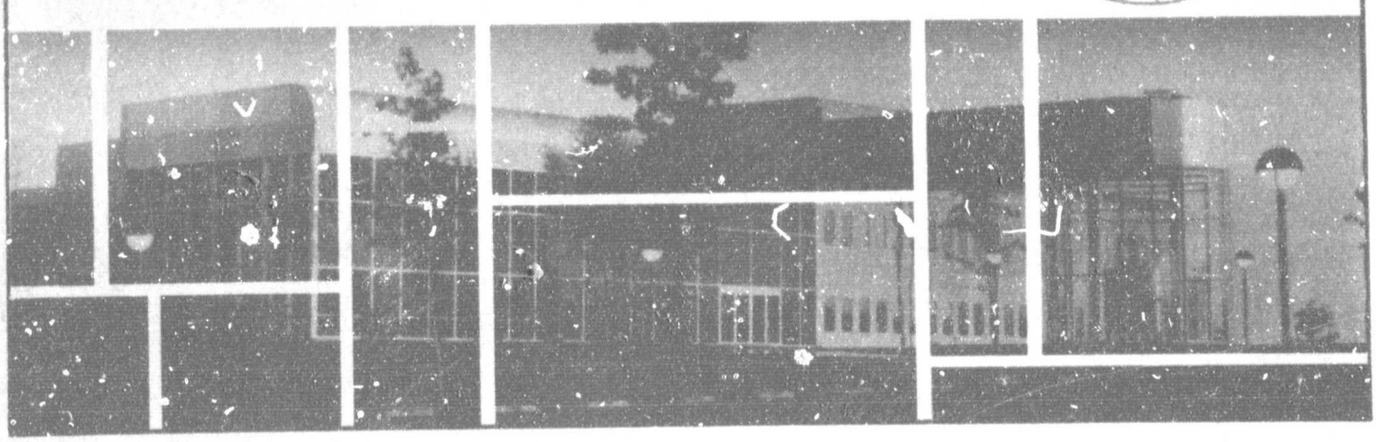

NASA
CR-159871

# FINAL REPORT

# THIN n-i-p RADIATION-RESISTANT SOLAR CELL FEASIBILITY STUDY

by

J. F. Allison, R. A. Arndt, A. Meulenberg, Jr.
COMSAT LABORATORIES

Prepared for

National Aeronautics and Space Administration
Lewis Research Center
Contract NAS3-21280

| 1. Report No. | 2. Government Accession No. | 3. Recipient's Catalog No. |
|---|---|---|
| NASA CR-159871 | | |

| 4. Title and Subtitle | 5. Report Date |
|---|---|
| Thin n-i-p Radiation-Resistant Solar Cell Feasibility Study | June 1980 |
| | 6. Performing Organization Code |
| 7. Author(s) | 8. Performing Organization Report No. |
| J.F. Allison, R.A. Arndt, A. Meulenberg, Jr. | |
| 9. Performing Organization Name and Address | 10. Work Unit No. |
| COMSAT Labs<br>22300 Comsat Drive<br>Clarksburg, MD 20734 | YJK7776 |
| | 11. Contract or Grant No. |
| | NAS3-21280 |
| 12. Sponsoring Agency Name and Address | 13. Type of Report and Period Covered |
| NASA-Lewis Research Center<br>21000 Brookpark Road<br>Cleveland, Ohio 44135 | Final Report |
| | 14. Sponsoring Agency Code |

15. Supplementary Notes

Program Manager, Dr. John C. Evans, Jr., NASA Lewis Research Center, 21000 Brookpark Road, Cleveland, Ohio 44135

16. Abstract

Silicon solar cells were fabricated to verify the predictions that: 1) thin $n^+pp^+$ cells can provide high values of open circuit voltage ($V_{oc}$) even when high resistivity base material (> 1000 Ω-cm) is used; 2) cells with good $p^+$ back contacts will display an increase in $V_{oc}$ with decreasing cell thickness; and 3) high quality, thin, high resistivity, solar cells can be made using processing compatible with conventional practice. Analysis of I-V and spectral response measurements of these cells confirmed theoretical predictions and thereby pointed to voltages beyond the near 600 mV obtained in this study.

| 17. Key Words (Suggested by Author(s)) | 18. Distribution Statement |
|---|---|
| Silicon solar cells<br>Radiation resistant<br>Thin cells<br>High Resistivity Cells | Unclassified - Unlimited<br>Star Category 44 |

| 19. Security Classif. (of this report) | 20. Security Classif. (of this page) | 21. No. of Pages | 22. Price* |
|---|---|---|---|
| Unclassified | Unclassified | | |

* For sale by the National Technical Information Service, Springfield, Virginia 22161

## ABSTRACT

Silicon solar cells were fabricated to verify the predictions that: 1) thin $n^+pp^+$ cells can provide high values of open circuit voltage ($V_{oc}$) even when high resistivity base material (> 1000 Ω-cm) is used; 2) cells with good $p^+$ back contacts will display an increase in $V_{oc}$ with decreasing cell thickness; and 3) high quality, thin, high resistivity, solar cells can be made using processing compatible with conventional practice. Analysis of I-V and spectral response measurements of these cells confirmed theoretical predictions and thereby pointed to voltages beyond the near 600 mV obtained in this study.

## SUMMARY

Theory predicts that the open circuit voltage of thin solar cells is not necessarily limited by the base resistivity. This study tested the feasibility of producing high performance, thin, $n^+pp^+$ solar cells with high resistivity ($\rho$ > 1000 Ω-cm) material and using processing compatible with conventional practice. The limiting factor was expected to be the effective surface recombination velocity (SRV) at the $p^+$ back contact. Several methods of producing this p+ back layer were tried and the most effective was the use of a spin-on boron dopant with overnight anneal. A series of cells ($\rho$ = 2, 10, 83, and 1250 Ω-cm) fabricated in this manner indicated an SRV of less than 1 cm/sec under low injection conditions.

Several sets of cells with variation in thickness (50 μm to 250 μm) indicated that voltage can increase with decreasing cell thickness. Limiting factors in the thin cells appear to be leakage across the $pp^+$ junction and bulk lifetime. Spectral response and I-V measurements at low levels and under illumination (up to AM0) from the $p^+$ or $n^+$ sides gave added information as to the influences of minority carrier injection at each junction and of series resistance due to the high resistivity bulk material.

The results of this study indicate that thin, high resistivity cells can achieve open circuit voltages near 600 mV

while maintaining good overall I-V characteristics. Cell voltages in excess of 650 mV appear feasible with AM0 power densities in excess of 21 $mW/cm^2$.

Table of Contents

List of Illustrations

List of Illustrations

List of Tables

# 1. INTRODUCTION

The conversion efficiency of silicon solar cells presently in use on satellites is significantly lower than the theoretical limit at beginning-of-life (BOL) and the loss of conversion efficiency due to the space radiation environment is greater than desired at end-of-life (EOL). These cells have been fabricated from p-type material with an $n^+$ diffused layer on the light incident side since this configuration is more radiation resistant than the $p^+$-n configuration. Resistivity of the base material typically ranges between 2 and 10 Ω-cm as a result of a trade-off between open circuit voltage which increases with decreasing resistivity and EOL short circuit current which decreases with decreasing resistivity.

The major cause of reduction of cell output at EOL is the loss of current collection efficiency resulting from degradation of bulk minority carrier lifetime. Recent improvements in current collection efficiency have been shown to be nearly independent of radiation level [1]. These are: (1), the use of a shallow $n^+$-p junction [2] (the Violet Cell) which increases the cell response to the violet end of the spectrum and (2), the use of a textured surface [3] (the CNR Cell) which reduces the overall reflectance of the cell. Addition of a $p^+$ back contact resulted in an increase of open circuit voltage at BOL [4] but this improvement disappears with increased radiation fluence in cells typically used on satellites.

It is well known that, as the resistivity of the bulk p-type silicon increases, the tolerance of carrier lifetime to radiation increases. Classical theory has shown that the open circuit voltage of a $n^+$-p cell decreases with increasing resistivity but, if a cell with a good $p^+$ back contact and long minority carrier diffusion length can be made, the open circuit voltage will increase with decreasing cell thickness. Therefore, a thin $n^+$-i-$p^+$ structure (for this study the symbol "i" is used to indicate high resistivity and/or intrinsic base material) should produce a high open circuit voltage cell which exhibits little loss of short circuit current under irradiation. The purpose of the work reported here was to prove the feasibility of fabricating such a cell.

## 2. THEORETICAL BACKGROUND

The theory leading toward demonstrating feasibility of a high efficiency, radiation-resistant silicon solar cell is presented below. Since high BOL current collection efficiency has already been demonstrated, the concern here is with reducing the potential for radiation induced degradation of the short circuit current ($I_{sc}$) but without sacrificing high open circuit voltage ($V_{oc}$).

### 2.1 SHORT CIRCUIT CURRENT

If the effects of surfaces are neglected and good optical matching is achieved, the major cause of short circuit current loss is recombination in the bulk of the solar cell. This recombination increases under irradiation and is mathematically described as a change in minority carrier diffusion length by

$$\frac{1}{L^2} = \frac{1}{L_o^2} + K_L \phi \qquad (1)$$

where $L_o$ and L are the diffusion lengths before and after irradiation with a fluence $\phi$ and $K_L$ is a proportionality constant that depends on the irradiating species, its energy and the material. The value of $K_L$ for 10 Ω-cm, p-type silicon under 1 MeV electron irradiation [5] is about $8 \times 10^{-11}$. If the data for $K_L$ as a function of resistivity are extrapolated to 1000 Ω-cm

silicon, a value of ~5 x $10^{-12}$ is obtained. This means that the onset of current loss will occur at a fluence level of nearly an order of magnitude greater in 1000 Ω-cm silicon than in 10 Ω-cm silicon and the rate of current loss will be less for the 1000 Ω-cm material.

It should be noted that the data from which the above extrapolation was made were obtained with no illumination of the cells during irradiation. In high resistivity material the carrier densities created by AM0 illumination are greater than the equilibrium densities (high injection) and $K_L$ may significantly differ from the extrapolated data. A further complication arises in that the diffusion lengths themselves are most probably dependent on injection level.

## 2.2 OPEN CIRCUIT VOLTAGE

The current density (J) in a solar cell is given by

$$J = J_d + J_r - J_\ell \qquad (2)$$

where $J_d$ is a reverse dark current from the bulk and diffused regions, $J_r$ is a reverse dark current from the junction regions, and $J_\ell$ is the photo-generated current. In most instances the $J_d$ term is much larger than the $J_r$ term which is therefore usually neglected. The $J_d$ term consists of two parts: one from the diffused region and one from the bulk region. It is common to neglect the part arising from the diffused region because of the

high doping level present there and consider only the part from the bulk region [6]. In this case $J_d$ becomes

$$J_d = J_{do} \left[\exp \frac{qV}{kT} - 1\right] \tag{3}$$

where

V = cell voltage
q = electronic charge
k = Boltzmann's constant
T = cell temperature (°K)

and

$$J_{do} = q \frac{n_{po} D_n}{L_n} \left[ \frac{s \cosh\left(\frac{W}{L_n}\right) + \frac{D_n}{L_n} \sinh\left(\frac{W}{L_n}\right)}{\frac{D_n}{L_n} \cosh\left(\frac{W}{L_n}\right) + s \sinh\left(\frac{W}{L_n}\right)} \right] \tag{4}$$

In Equation 4, the symbols have the following meaning:

$n_{po}$ = equilibrium electron concentration in the bulk (p-type)

$D_n$ = electron diffusion constant in bulk

$L_n$ = electron diffusion length in the bulk

W = thickness of bulk region

s = effective surface recombination velocity at the back contact (or p-$p^+$ junction).

In cells with ohmic back contacts $s >> D_n/L_n$ and the term in brackets in equation (4) becomes coth $(W/L_n)$. In this case $J_{do}$ increases with decreasing cell thickness. Irrespective of the value of s compared to $D_n/L_n$ the open circuit voltage depends

upon $J_\ell$ and $J_{do}$ as (solving equation (2) and equation (3) for J = 0)

$$V_{oc} = \frac{kT}{q} \ell n \left( \frac{J_\ell}{J_{do}} + 1 \right), \tag{5}$$

provided $J_r$ is neglected.

It has been known for sometime that the addition of a $p^+$ layer to the p-type base would result in a minority carrier reflecting property [7]. Godlewski et al. [8] applied this principle to solar cells and arrived at the following expression for the effective surface recombination velocity:

$$s = \frac{N_A}{N_A^+} \frac{D_n^+}{L_n^+} \left[ \frac{s_n \cosh\left(\frac{W^+}{L_n^+}\right) + \frac{D_n^+}{L_n^+} \sinh\left(\frac{W^+}{L_n^+}\right)}{\frac{D_n^+}{L_n^+} \cosh\left(\frac{W^+}{L_n^+}\right) + s_n \sinh\left(\frac{W^+}{L_n^+}\right)} \right] \tag{6}$$

In Equation 6, $N_A$ and $N_A^+$ are the acceptor densities in the p and $p^+$ regions, respectively, $s_n$ is the actual surface recombination velocity at the $p^+$ surface, and the plus superscripts indicate the parameters applying to the $p^+$ region. One can see from equation (6) that, for a given base layer doping density, the value of s decreases with increasing doping density in the $p^+$ layer. The addition of the $p^+$ layer on solar cells produces what is known as the back surface field (BSF) and is responsible for reducing s. If $s << D_n/L_n$ the term in brackets in equation (4) becomes tanh $W/L_n$ and, for very small values of $W/L_n$, tanh $(W/L_n)$ approaches $W/L_n$. In this case

$$J_{do} = q\left(\frac{n_{po}\, D_n}{L_n}\right)\left(\frac{W}{L_n}\right) = q\,\frac{n_{po}\, W}{\tau_n} \qquad (7)$$

where $\tau_n$ is the minority carrier lifetime in the bulk. Reduction of the cell thickness results in a direct reduction of $J_{do}$ and an increase in $V_{oc}$ according to equation (5), providing the value of $J_\ell$ does not change. The derivation will not be repeated here but it has been shown [9] that, as the bulk region approaches intrinsic character, $J_d$ becomes

$$J_d = \frac{2q\, n_i\, W}{\tau}\left[\exp\left(\frac{qV}{2kT}\right) - 1\right] \qquad (8)$$

where V is the terminal voltage and $n_i$ is the intrinsic carrier concentration. The value of $J_{do}$ for intrinsic material is greater than for extrinsic p-type material due to the increase in the equilibrium electron concentration ($n_{po}$ approaches $n_i$). However, the factor of two in the denominator of the exponent of equation (8) compensates for this and high values of $V_{oc}$ are still attainable. For example, if W = 50 μm and τ = 500 μsec, the value of $V_{oc}$ for $J_\ell$ = 40 mA/cm$^2$ is about 700 mV. In intrinsic material, changes in the value of τ should not be as sensitive to radiation as in low resistivity material and, therefore, $J_{do}$ will not be as sensitive to radiation.

The above description is the basis for performing research on thin, n-i-p solar cells.

# 3. EXPERIMENTS AND RESULTS

The basic goal of this study was to demonstrate the feasibility of fabricating solar cells from high resistivity base material that exhibit good $p^+$ back characteristics and maintain reasonably high open circuit voltage and current-voltage curve fill factors. The principles set forth in Section 2 were used as a guide in performing experiments designed to meet this goal. In addition to the fabrication of cells, some modeling was undertaken to explain some of the experimental results.

## 3.1 $p^+$ BACK FORMATION

In keeping with the theory, equation (6), in which it was shown that a lower effective surface recombination velocity can be achieved if the doping concentration in the $p^+$ region is as high as possible, boron doping was used to form the $p^+$ layer. Boron has an advantage over aluminum for this purpose because its solid solubility in silicon is greater than that of aluminum at the temperatures normally used for diffusion. A comparison of current-voltage curves, obtained under AM0 illumination, of cells with $p^+$ backs of boron and aluminum, but otherwise identically fabricated, is shown in Figure 3-1.

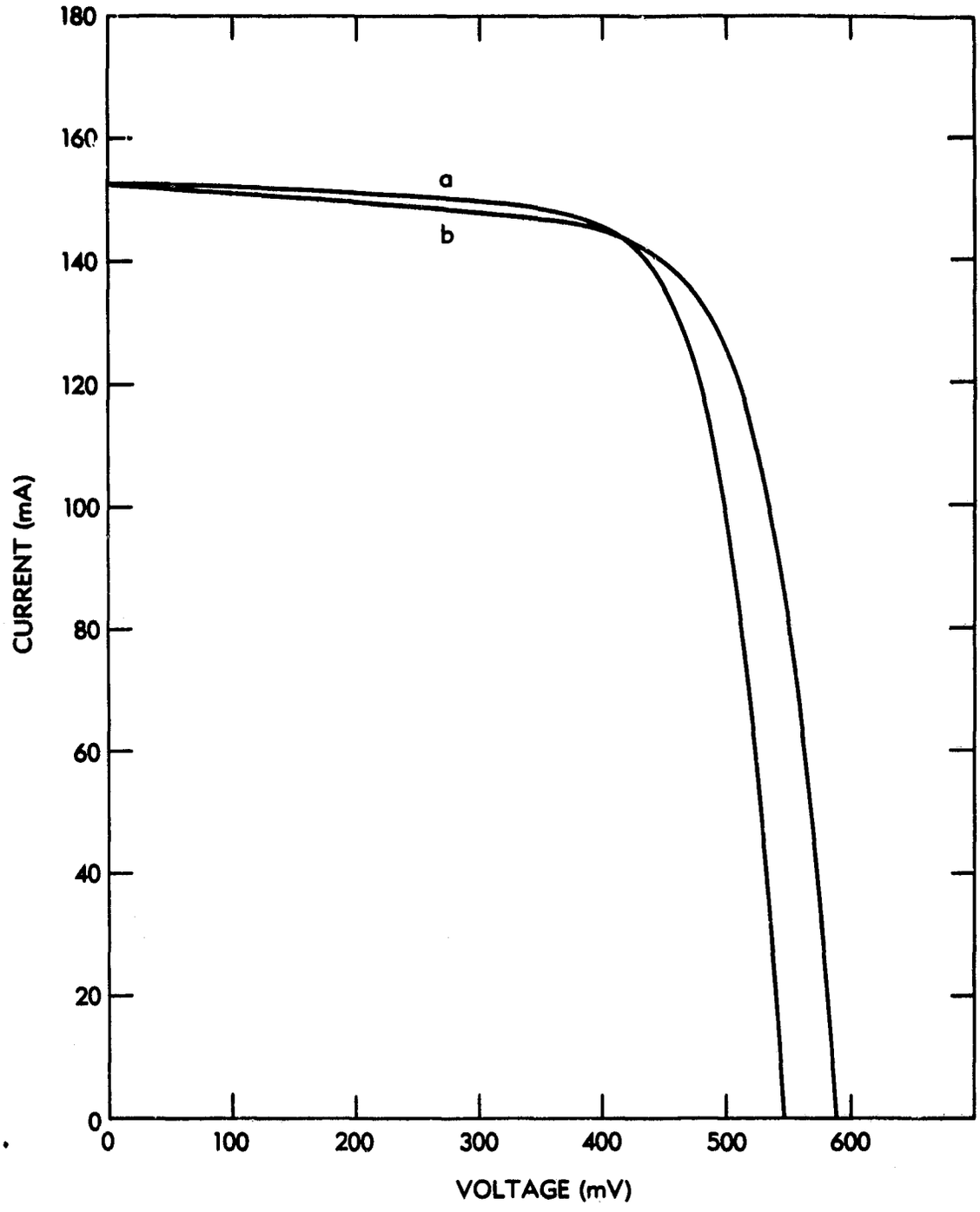


Figure 3-1. Current-Voltage Curves of 4 $cm^2$ Solar Cells Fabricated with Aluminum Alloy (a), and Borosilicafilm 0317 (b), Back $p^+$ Junctions

Several methods have been attempted for forming the boron $p^+$ back by diffusion*. The sources included: (1) a gaseous $BCl_3$, (2) boron doped CVD silica, (3) solid wafers of $B_2O_3$, and (4) spin-on films (Emulsitone Borosilica film 0317). All sources except the spin-on films yielded cells with reduced carrier lifetime in the bulk. Several annealing treatments were tried in an effort to improve the bulk carrier lifetime. Only the spin-on films yielded cells with satisfactory carrier lifetimes when the diffusion process was followed by an overnight anneal at 450°C in forming gas. Figure 3-2 shows the current-voltage curves under AM0 illumination for 250 μm thick cells of 10 Ω-cm base resistivity with and without the 450°C anneal.

An assessment of the quality of $p^+$ backs using boron was made. For example, a 250 μm thick cell made from 10 Ω-cm silicon was measured under AM0 illumination and the following results obtained: $I_{sc}$ = 39.9 mA/cm$^2$ and $V_{oc}$ = 602 mV. In 10 Ω-cm material, AM0 illumination should not be intense enough to create a minority carrier density much greater than the equilibrium concentration of the majority carriers and equation (3) should

*Many of these had already been tried at COMSAT Laboratories before the inception of work on this contract. It was deemed unnecessary to repeat these experiments since they generally yielded poor results.

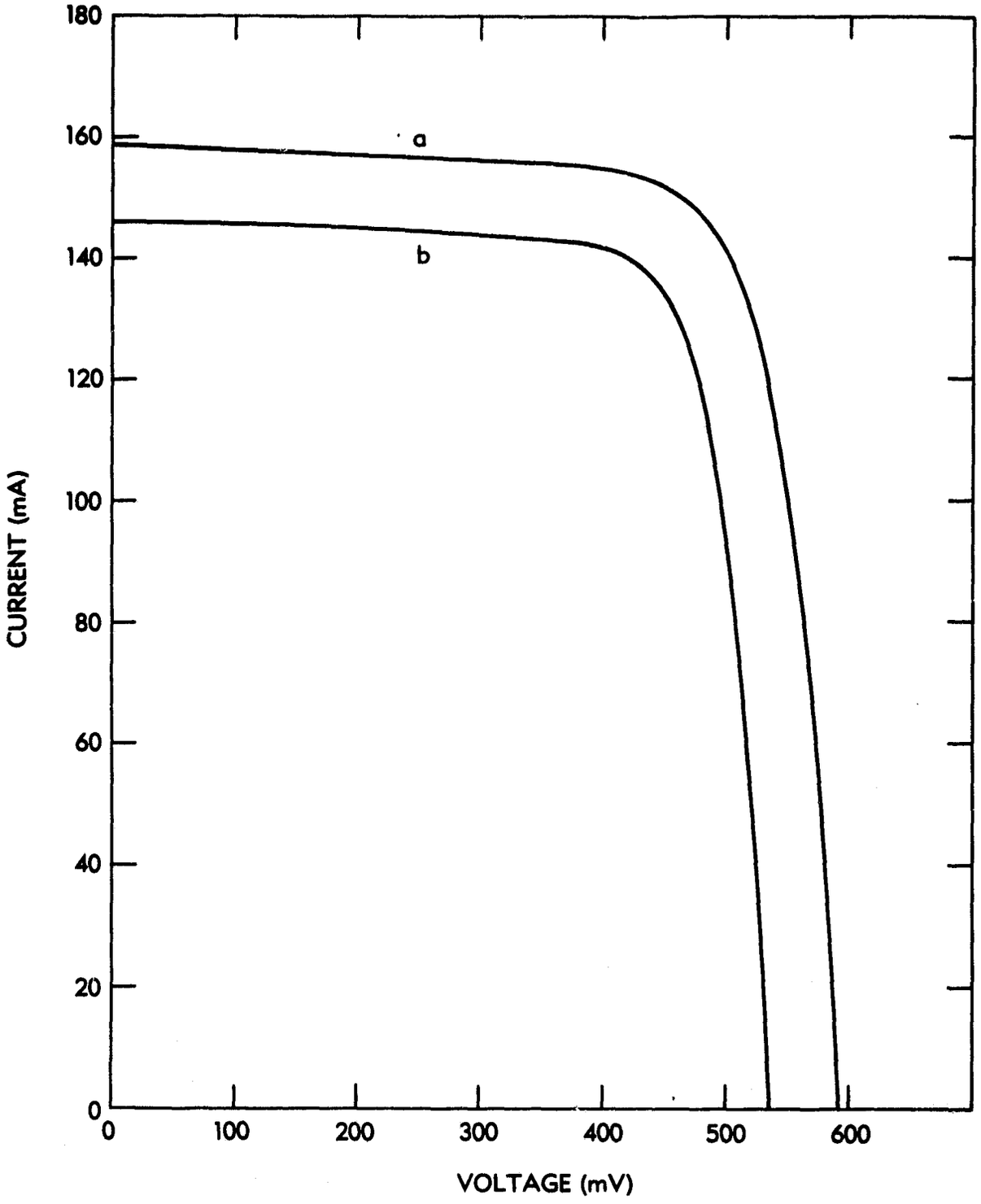


Figure 3-2. Current-Voltage Curves of 4 $cm^2$ Solar Cells Fabricated with Borosilica Film 0317 Illustrating Improvement in Cell Characteristics Due to 450°C-16 hr Anneal in Forming Gas (90% $N_2$ - 10% $H_2$) a) with Anneal b) without Anneal

be applicable. The computed value of $J_{do}$ is $2.67 \times 10^{-12}$ A/cm$^2$. Inserting this value into equation (4) and assuming $D_n$ = 35 cm$^2$/sec, one can compute combinations of values for $L_n$ and s by letting $L_n$ vary and finding the corresponding value for s. The results are:

| $L_n$ (μm) | s (cm/sec) |
|---|---|
| 850 | 0 |
| 1000 | 17 |
| 1250 | 54 |
| 1500 | 68 |
| 1750 | 100 |

If the effective surface recombination velocity is greater than 100 cm/sec the diffusion length would have to be uncommonly long for 10 Ω-cm material and, therefore, it is concluded that the value of s is less than 100 cm/sec and probably less than 10 cm/sec.

An added advantage of using boron as the dopant for forming $p^+$ back surfaces is that the boron does not roughen the surface as does the use of aluminum. This leaves a polished surface with a high degree of specular reflection and subsequent application of a back surface reflector (BSR) is very effective in reducing the absorptance of the cell. One cell was fabricated with a BSR of evaporated aluminum and the absorptance of the cell (250 μm thick) was 0.73. The reflectance measured at 1.5 μm was 85 percent, a value very near to the theoretical value.

## 3.2 THICKNESS DEPENDENCE OF $V_{oc}$

In the case described in subsection 3.1, the condition $s << D_n/L_n$ is certainly met if $L_n$ = 1000 μm but if $L_n$ = 1750 μm the value of s is only one-half the value of $D_n/L_n$. Figure 3-3 shows a plot of the bracketed term in equation (4) as a function of $W/L_n$ for various values of $sL_n/D_n$. It can be seen that a reduction of $W/L_n$ by a factor of two does not necessarily result in a reduction of $J_{do}$ by a factor of two. Furthermore, the limiting value of the term in backets in equation (4) is $sL_n/D_n$ as $W/L_n$ approaches zero and $J_{do}$ approaches $qN_{po}s$.

Several sets of cells were fabricated with different resistivity and thickness in an attempt to demonstrate increased $V_{oc}$ with decreasing thickness. In low resistivity cells (~10 Ω-cm) the open circuit voltage did not show any definite trend toward increasing as the thickness decreased. In higher resistivity cells (83 Ω-cm and 1250 Ω-cm), although there is a great deal of scatter, there is a trend toward increasing $V_{oc}$ with decreasing thickness and this is shown in Figure 3-4. Also shown in Figure 3-4 are computed values of $V_{oc}$ obtained by using Equations 4 and 5, a value of D = 35 $cm^2/sec$, and assuming that $J_\ell$ does not change with cell thickness. Both curves are based on a value of 558 mV for 250 μm and the parameters are:

| | $sL_n/D_n$ | $L_n$ |
|---|---|---|
| Curve 1 | 0.3 | 1500 |
| Curve 2 | 0.2 | 1250 |

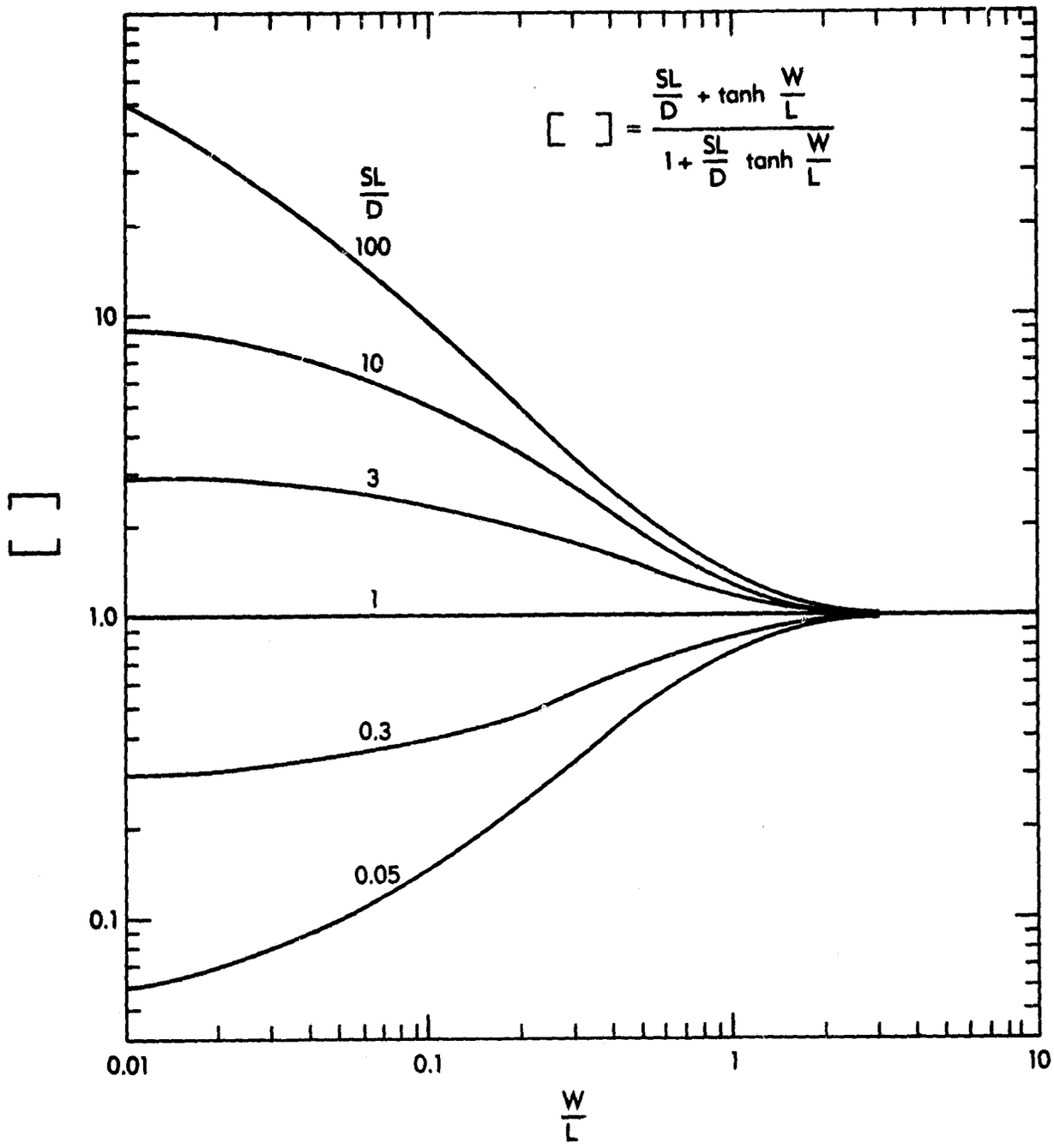


Figure 3-3. Plot of Bracketed Term in Equation 4 vs the Cell Thickness with Respect to the Diffusion Length as a Function of the Relative Surface Recombination Velocity sL/D

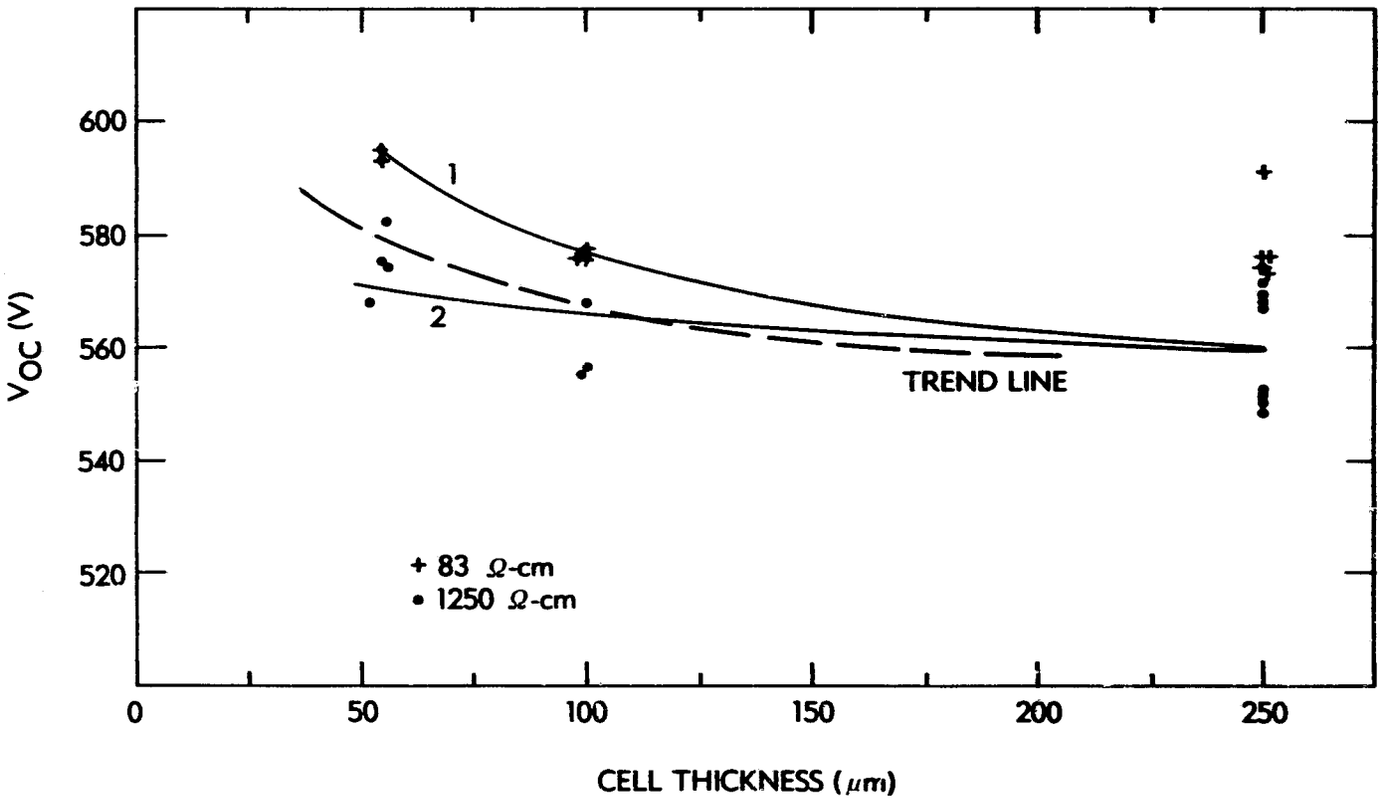


Figure 3-4. Plot of $V_{oc}$ vs Cell Thickness Showing Experimental Trend of Increasing $V_{oc}$ with Decreasing Thickness (Dashed line) and Computed $V_{oc}$ (see text for parameters of curves 1 and 2)

## 3.3 GRID BACK CONTACTS

Several cells were made with grid contacts on the back ($p^+$ side) as well as on the front ($n^+$ side) sides of the cells. One advantage of such a structure with small amounts of metal coverage is that most of the light of energy less than the optical band gap will pass through the cell and not contribute to the absorptance. A second advantage is that cells made from 1250 Ω-cm material exhibited higher open circuit voltage and better fill factor when illuminated on the $p^+$ side than when illuminated on the $n^+$ side. This effect is shown in Figure 3-5 and discussed below.

In a cell made from high resistivity (~1000 Ω-cm) p-type material, a significant portion of the terminal voltage of the cell is developed across the p-$p^+$ junction. Because the light from AM0 illumination does not generate carriers uniformly throughout the bulk region, the back (p-$p^+$) junction may or may not be in high injection conditions at low cell voltages and the voltage developed across the p-$p^+$ junction will depend on cell thickness. In addition, for thick (250 μm) cells there is a significant Dember voltage developed across the bulk region that is in the opposite sense of the junction potentials when the illumination is on the $n^+$ side. When the cells are illuminated on the $p^+$ side the roles of the two junctions are reversed and the sense of the Dember voltage is the same as the junction

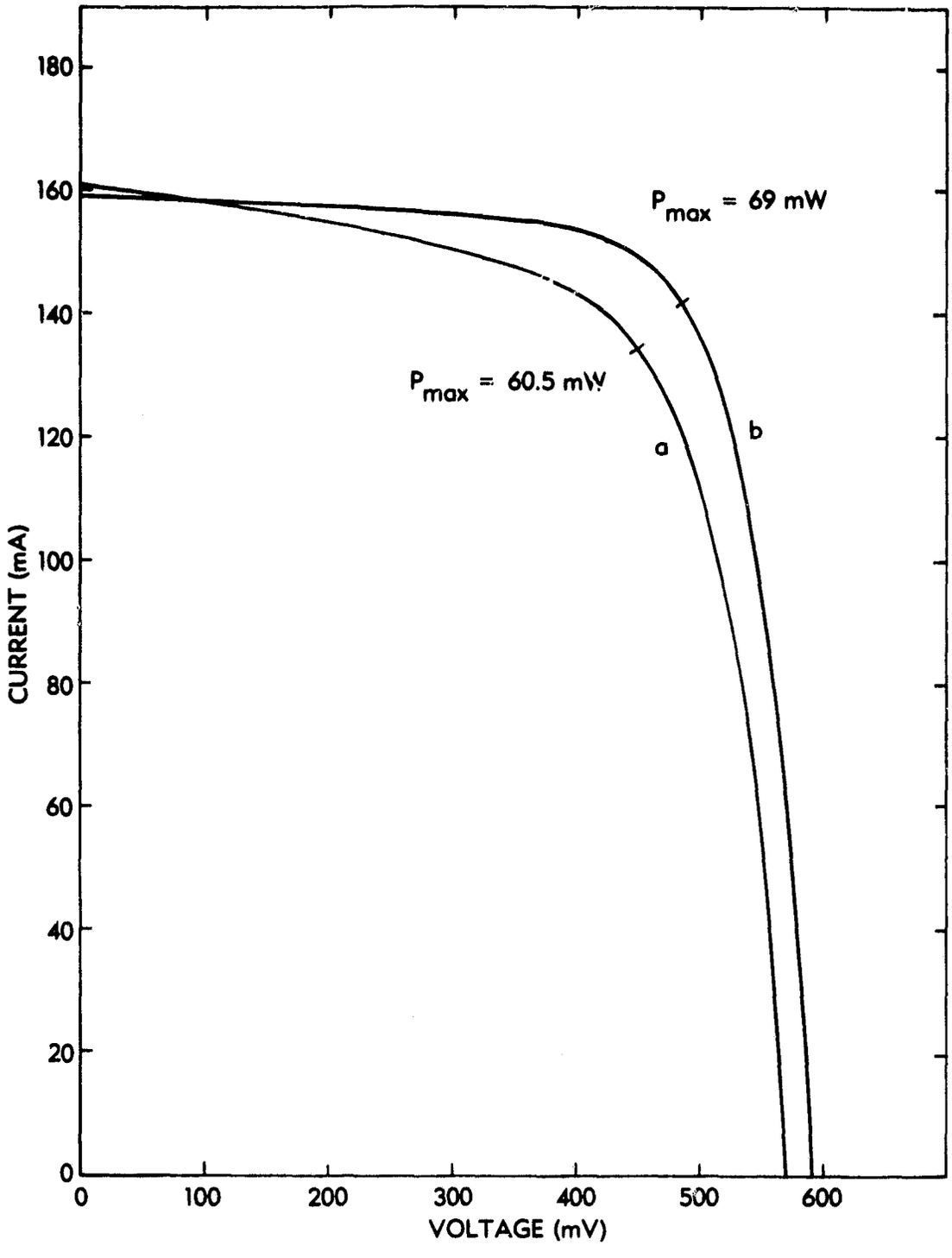


Figure 3-5. Current-Voltage Curves of 4 $cm^2$ Solar Cell, 250 μm Thick, Under AM0 Forward ($n^+$-p) Illumination (a) and Rear ($p^+$-p) Illumination (b) Showing Improvement in $V_{oc}$ and Fill Factor Under Rear Illumination

voltages but the magnitude will be much less. Similar results have been reported elsewhere [10] and further discussion appears in Section 3.5.

The basic equations for n-i-p solar cells under non-uniform carrier generation have been set up in a manner similar to that of Sabnis [11] who set them up for uniform generation. These equations take a form similar to equation (3) where, now, the voltages across both junctions are included as well as the voltage dependence of the reverse currents (see Appendix B for a complete description). For the cell fabricated from 1250 Ω-cm material, the open circuit voltage when illuminated with AM0 light was about 10 mV higher with $p^+$-side illumination than with $n^+$-side illumination. When tungsten light (~3000 K) of intensity sufficient to produce the same short circuit current as the AM0 light was used, the $V_{oc}$ for the $p^+$-side illumination was 60 mV greater than for $n^+$-side illumination. These differences in front and rear illuminated $V_{oc}$ for the different spectrums are within one millivolt of those calculated.

## 3.4 SPECTRAL RESPONSE

While the primary measurement of solar cell performance is the AM0 illuminated current-voltage characteristic, much information can be obtained by examining the spectral response and the internal quantum efficiency of the cells.

This study used the alloyed aluminum $p^+$ back formation technology as a base line from which an improved $p^+$ back was developed. The quantum efficiencies, under low level illumination, for 1, 10, 30, and 1250 Ω-cm cells, 250 μm thick, with aluminum $p^+$ backs are shown in Figure 3-6. The values at short wavelengths are low because a reliable, but moderately deep, $n^+$ layer was used so that any irregularities that may occur at this surface would not significantly affect the study of the $p^+$ back. The red response of the 1 Ω-cm sample was low due to lower diffusion length and reduced effectiveness (equation 6) of the $p^+$ back layer.

Cells (250 μm thick) fabricated from 83 and 1250 Ω-cm material and with boron $p^+$ backs and grid contacts were also measured under low level illumination (short circuit currents equal to about 1 percent of those obtained under AM0). The quantum efficiency in the central portion of the spectrum of a 83 Ω-cm cell (Figure 3-7), when illuminated on the $p^+$ side, was only about one-half that obtained when the illumination was on the $n^+$ side. If it is assumed that the only carrier losses occur in the bulk of the cell (s = 0), a minimum diffusion length can be estimated from the relative differences in quantum efficiency in the 500 to 800 μm wavelength range under $n^+$-p and $p^+$-p surface illumination. Since the absorption coefficient for this light is $>10^3$ $cm^{-1}$, all carriers are essentially generated at the illuminated

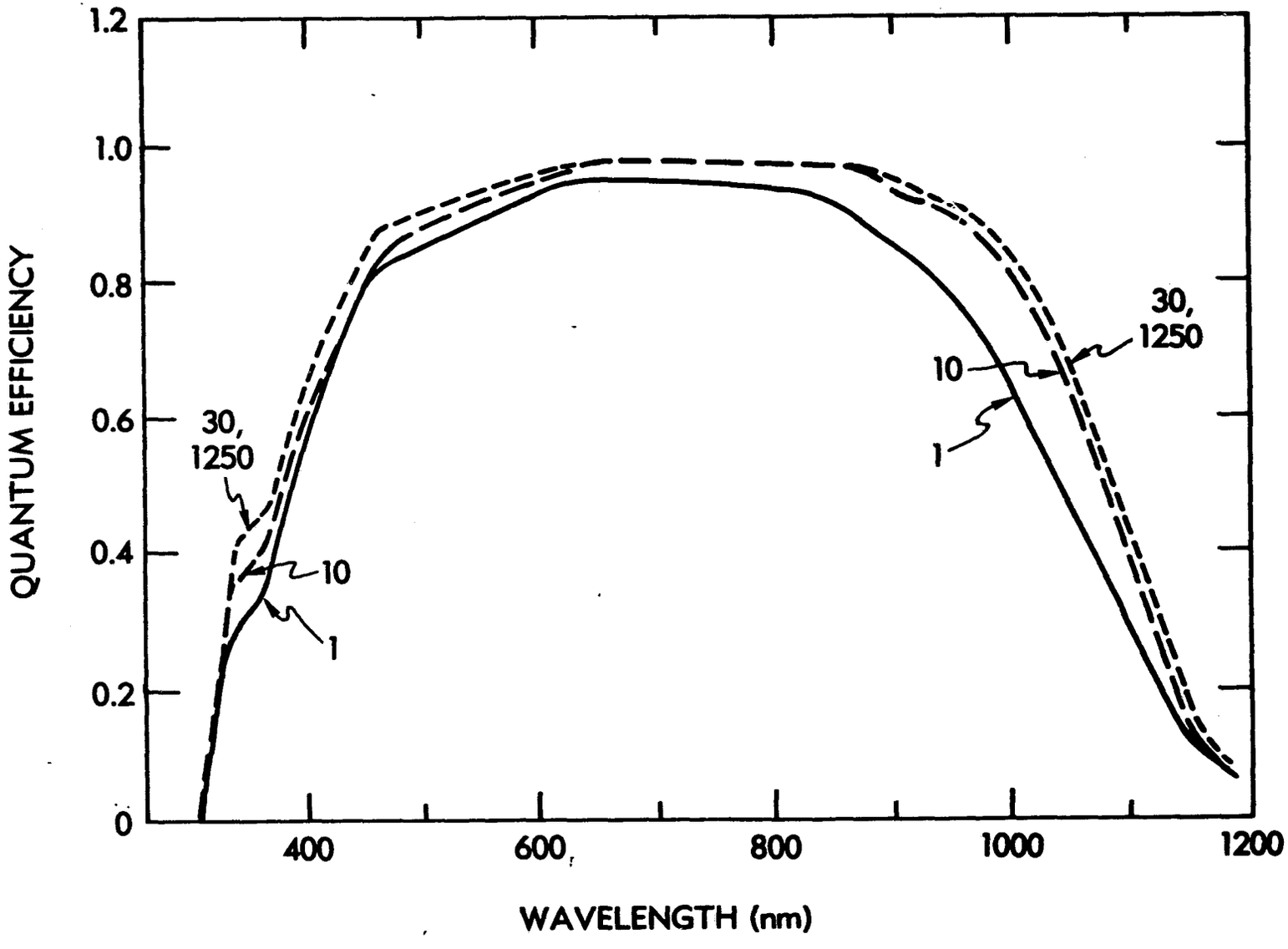


Figure 3-6. Internal Quantum Efficiency as a Function of Wavelength at Low Level Illumination for 1, 10, 30, and 1250 Ω-cm Cells Fabricated with Al Alloy Back Contacts

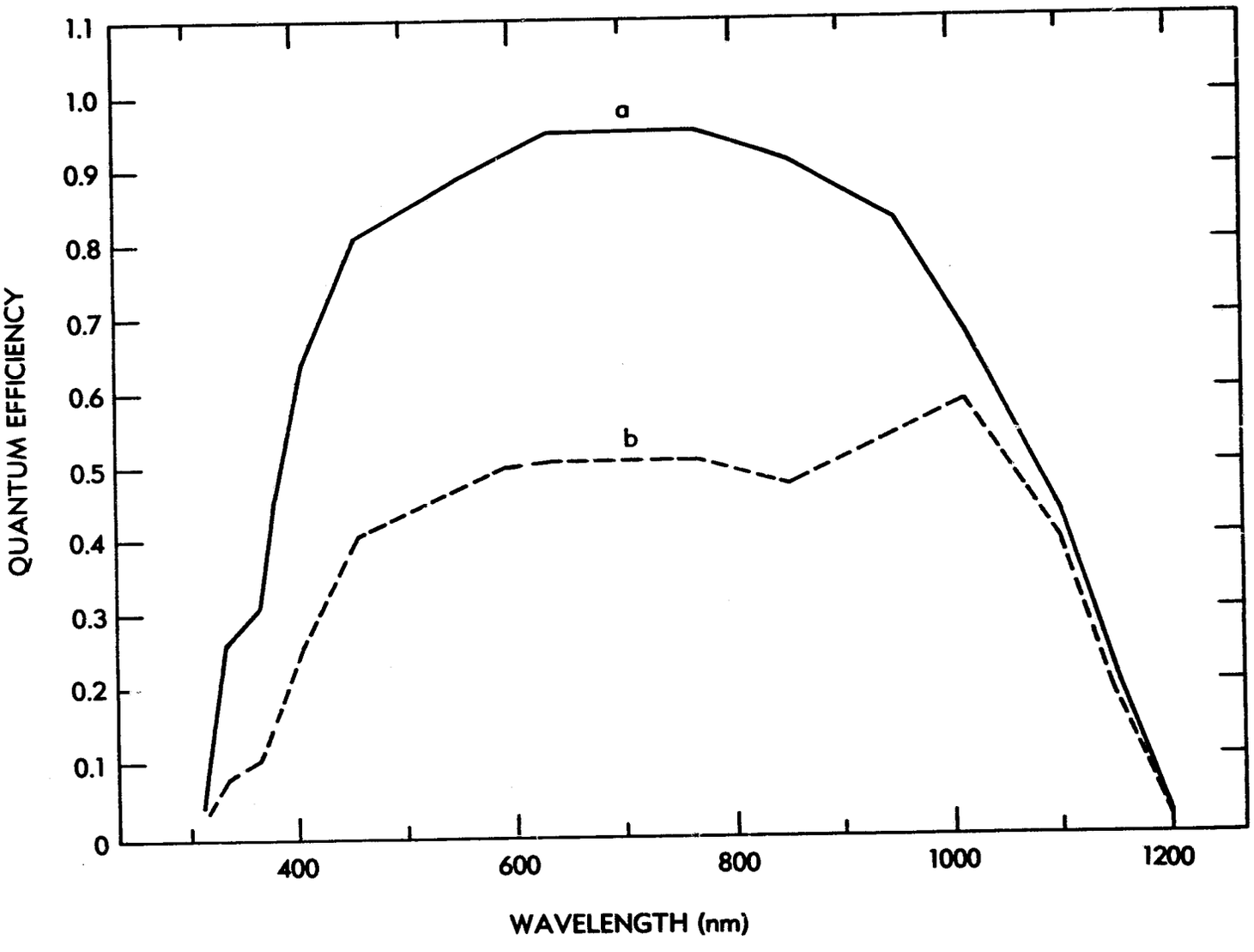


Figure 3-7. Internal Quantion Efficiency as a Function of Wavelength Low Level Illumination for 83 Ω-cm, 250 μm Thick $n^+$-p Cell, as Measured from the Front ($n^+$-p) Side (a) and Read ($p^+$-p) Slide (b)

surface. Under $p^+$-p illumination the generated carriers must travel through the entire cell to the $n^+$-p junction to be collected. The ratio of quantum efficiencies can then be expressed as

$$\frac{Q_B}{Q_F} = e^{-\left(\frac{W}{L_n}\right)} \qquad (9)$$

It can thus be estimated that this 83 Ω-cm cell has a minimun diffusion length of 350 μm. The response at wavelengths less than 450 nm is significantly less when the illumination is on the $p^+$ side than on the $n^+$ side indicating a surface layer on the $p^+$ side with a short lifetime. The quantum efficiency of a similarly fabricated cell of 1250 Ω-cm resistivity is shown in Figure 3-8. The short wavelength response is low for illumination on either side. In this case, however, the response (500-800 nm) when the $p^+$ side is illuminated is about 90 percent of that for the $n^+$ side. The diffusion length is thus in excess of 2350 μm.

A series of spectral response measurements taken at differing light bias illumination levels was quite revealing. In this method "chopped" low level monochromatic light is used to illuminate the cell simultaneously with light from the solar simulator. Neutral density filters are used to vary the intensity from the simulator. The signal from the chopped light is detected with a tuned amplifier. Cells fabricated on 2, 10, 83, and 1250 Ω-cm p-type silicon were measured at wavelengths of 404.7 nm,

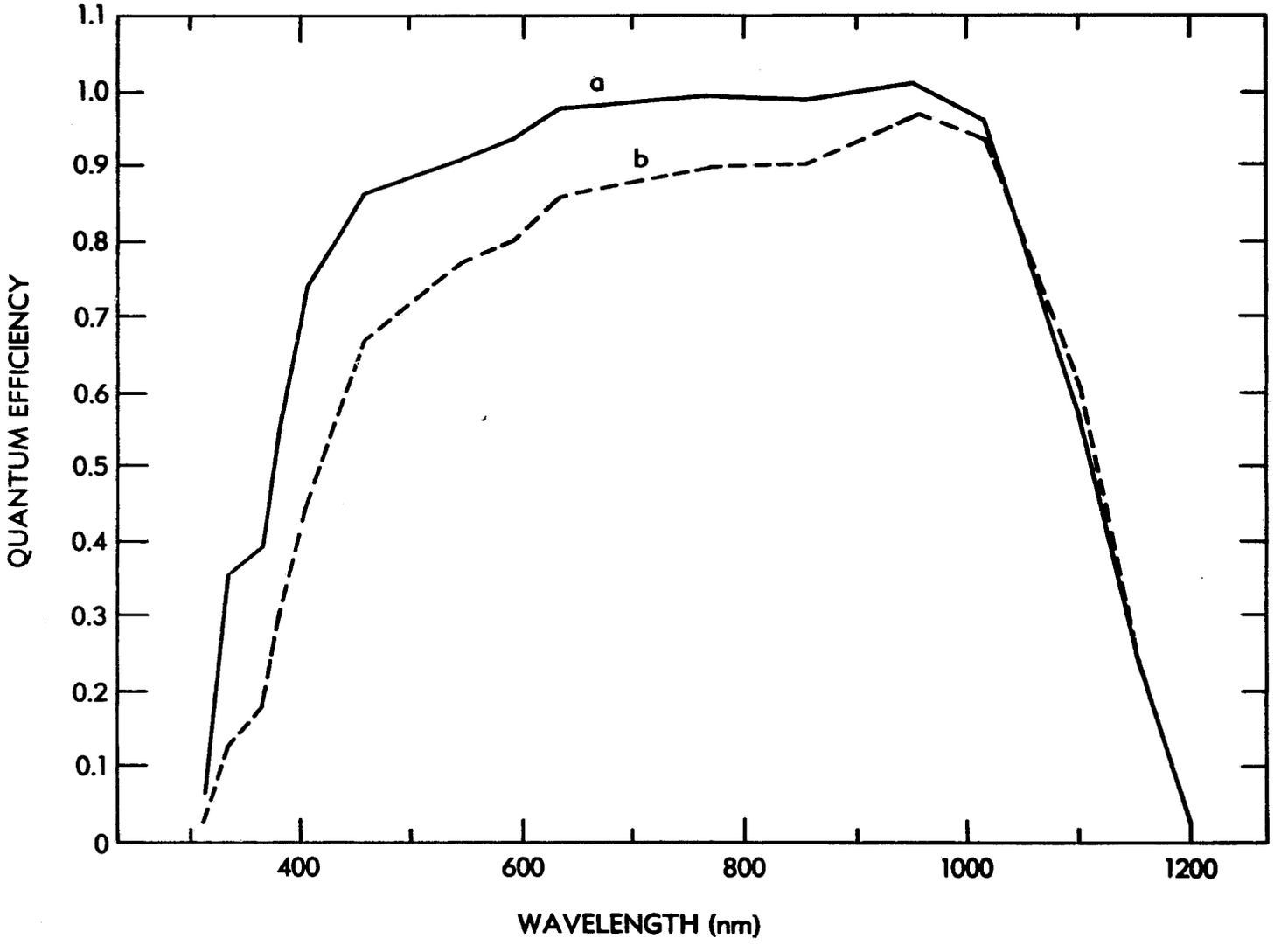


Figure 3-8. Internal Quantum Efficiency as a Function of Wavelength at Low Level Illumination for $n^+$-p 12500 Ω-cm, 250 μm Thick Cell as Measured From the Front ($n^+$-p) Side (a), and the Read ($p^+$-p) Side (b)

632.8 nm, and 950.0 nm under light bias levels of 10, 30, and 100 percent AM0. Table 3.1 contains these data in the form of percent increase (+) or decrease (-) from the zero bias light level. The measurement error is estimated to generally be ±5 percent except under AM0 bias when ±10 percent was experienced. The 1250 Ω-cm cell was measured with illumination incident on, first, the front ($n^+$) and then the back ($p^+$) surface.

The data in Table 3.1 show the major variations occurring in the high resistivity (1250 Ω-cm) cell at high bias levels. The strong drop in response at 404.7 nm under the AM0 bias condition, can be accounted for only by a reduction in collection of carriers generated in the $n^+$ region. Since the dopant concentration in this region is very high, the lifetime is not influenced at this illumination level and the reduced collection is probably due to a reduction in the electric field in the $n^+$ layer. This field, produced by the junction field and the concentration gradient from the diffusion profile, is reduced as the cell voltage increases (hence reducing the junction potential). In high resistivity cells, a drop in front junction potential could be experienced when illumination raises the IR drop across the bulk region and forward biases the front junction. In such a case, the potential across the junction is significantly reduced as the IR drop may exceed 400 mV.

Table 3.1. Injection Level Effects on Spectral Response

| λ(nm) | ρ(Ω-cm) | 10% | 30% | 100% AM0 |
|---|---|---|---|---|
| 404.7 | 2 | 0 | 0 | 0 |
| | 10 | 0 | 0 | 0 |
| | 83 | +2 | 0 | 0 |
| | 1250F | 0 | | -40 |
| | 1250B | 0 | | -20 |
| 632.8 | 2 | +8 | +2 | +4 |
| | 10 | 0 | -4 | +16 |
| | 83 | 0 | +4 | +13 |
| | 1250F | -3 | | -56 |
| | 1250B | -3 | | -7 |
| 950.0 | 2 | +6 | -6 | 0 |
| | 10 | 0 | 0 | 0 |
| | 83 | +5 | -3 | -9 |
| | 1250F | 0 | | -27 |
| | 1250B | -7 | | -10 |

Since collection of carriers generated in the $n^+$ region is strongly influenced by an electric field, a reduction of this field by up to a factor of two could easily account for the 40 percent blue current drop observed in the 1250 Ω-cm cell. This effect could also cause the slope in the I-V characteristic often seen in high resistivity cells when illuminated from the front.

The second result of the light bias is in a lowered red response in the 1250 Ω-cm cells and is attributed to a reduction in bulk diffusion length. A change in diffusion length with illumination is expected for most cells fabricated in moderately doped (≅10 Ω-cm) silicon [12]. Illumination can raise the carrier concentrations such that charged defect levels become neutralized and therefore can increase the lifetime (τ). In higher resistivity

cells (≧100 Ω-cm), one sun illumination can create high injection even near the short circuit current operating point. This nullifies the influence of many defects and maximizes the lifetime. However, since the ambipolar diffusion coefficient (D*) is lower than that for electrons ($D_n$), the resulting diffusion length is somewhat lower than the increased $\tau$ would tend to indicate ($L = \sqrt{D^*\tau}$). In very high resistivity material (1000 Ω-cm), the Fermi level is already above most defect levels and $\tau$ does not increase significantly with illumination level. Therefore, L will actually decrease with illumination as $D_n \rightarrow D^*$. The actual carrier concentration balance under high injection is determined by migration to the junctions (which depends on the cell voltage) and by the carrier lifetimes. However, the lifetimes are influenced by the number and charge state of deep defects dominating recombination [12]. Therefore, a complicated relationship exists between diffusion length, injection level, cell voltage, principle defect levels, and charge state.

The 27 percent loss in 950.0 nm generated current under AM0 illumination for the 1250 Ω-cm cell could correspond to a reduction in L by at least a factor of 5 and is therefore expected to be caused by more than just the transition to ambipolar conditions. The defect(s) hypothesized to cause the additional loss in L do not appear constant in all 1250 Ω-cm cells fabricated and may be dependent upon impurity gettering or

introduction during processing. The 56 percent loss in 632.8 nm light generated current at AM0 appears to be a combination of the losses from light generated in the $n^+$ layer and losses from reduced bulk diffusion length. If the bulk lifetime is dependent upon carrier concentration, then L could, in fact, be lower near the front of the cell than near the back surface. Likewise, thinner cells would have a shorter L than otherwise identical thick cells. This does fit some observed trends and would account for the scatter in the $V_{oc}$ versus cell thickness curve (Figure 3-4).

A third effect is the loss in 404.7 nm generated current with illumination from the back ($p^+$) contact. This is attributed in part to the reduction of the $p^+p$ potential by high injection. The rest of the loss at 404.7 nm and the losses in 632.8 nm and 950.0 nm response at high injection would be from the reduction in diffusion length. This cell under tungsten light illumination, displayed much lower than expected voltages for both front and rear illumination. The long wavelength light generates much higher carrier concentration within the cell bulk, particularly from front illumination; therefore the negative injection level effect would be much greater and the resulting low values of $L_n$ would give low values of $V_{oc}$ (see Appendix B).

## 3.5 I-V ANALYSIS

A dominant n = 2 component in the diode equation,

$$J = J_o \left[\exp\left(\frac{qV}{nkT}\right)-1\right] - J_\ell, \qquad (9)$$

is a predicted characteristic of intrinsic and high injection operation. In order to understand the operating mode of an experimental solar cell, it is necessary to analyze the illuminated I-V curve. Analysis has shown that, in low resistivity cells (~1 Ω-cm), the modes of operation in the dark and under illumination are nearly identical, indicating the validity of "superposition." In moderately high resistivity material (100-10,000 Ω-cm), dark I-V curves do not exhibit intrinsic operation but, under AM0 illumination, the electron and hole populations become more equal and a marked difference is seen between the dark and illuminated I-V characteristics (Figure 3-9 and 3-10). As the portion of the bulk nearer the illuminated surface approaches intrinsic operation, recombination in this region shifts the dark current from the n = 1 ($J_1$) component of extrinsic operation to the n = 2 ($J_2$) component of intrinsic or high injection operation. As seen in Figures 3-9 and 3-10 for an 83 Ω-cm cell, $J_1$ dropped by nearly a factor of five and $J_2$ increased by more than a factor of two. Results for 1250 Ω-cm, 250 μm thick cells (Figures 3-11 and 3-12) show an increase in $J_2$ by a factor of four and a decrease in $J_1$ by more than an order of magnitude under AM0 illumination. These

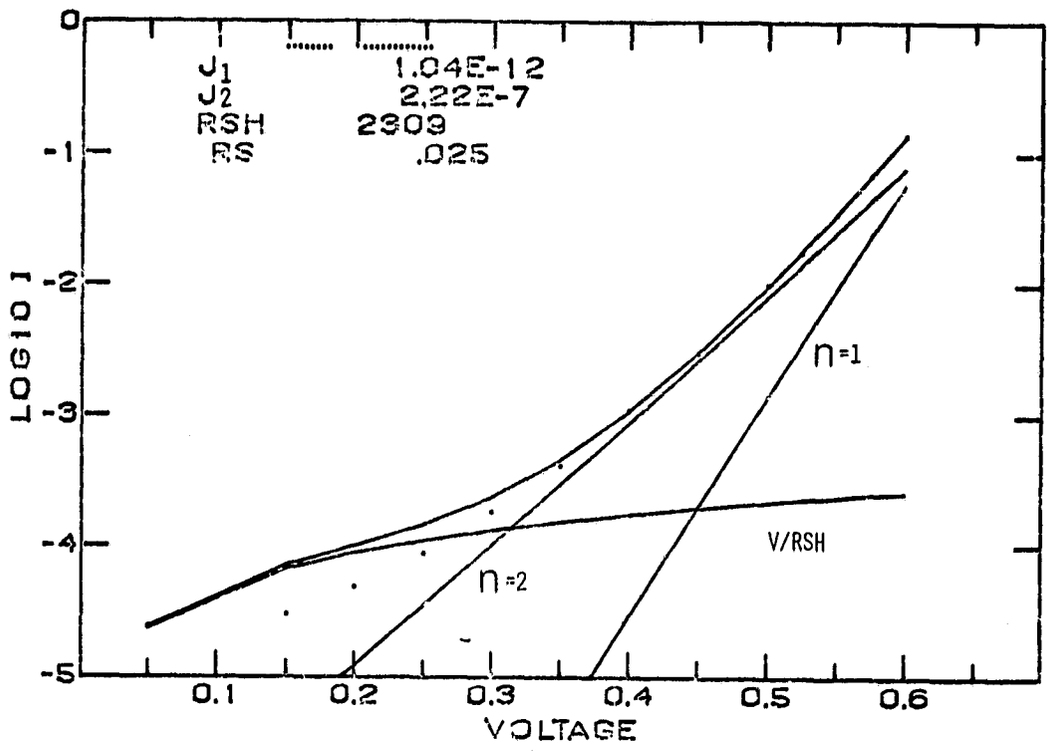


Figure 3-9. Dark IV Curve of an 83 Ω-cm $n^+pp^+$ Cell Along with the N = 1, N = 2 and Shunt Leakage Current Components. Dots are Experimental Data

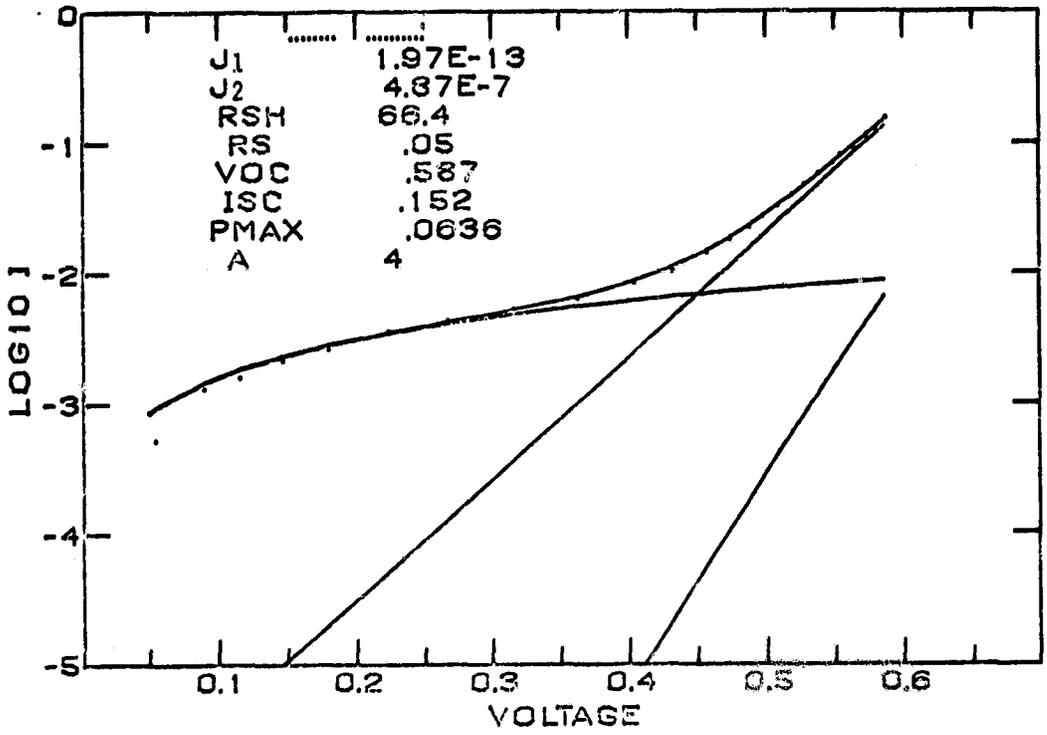


Figure 3-10. Illuminated IV Curve (Minus $I_{sc}$) for the Cell in Figure 3-9. Dots are Experimental Data

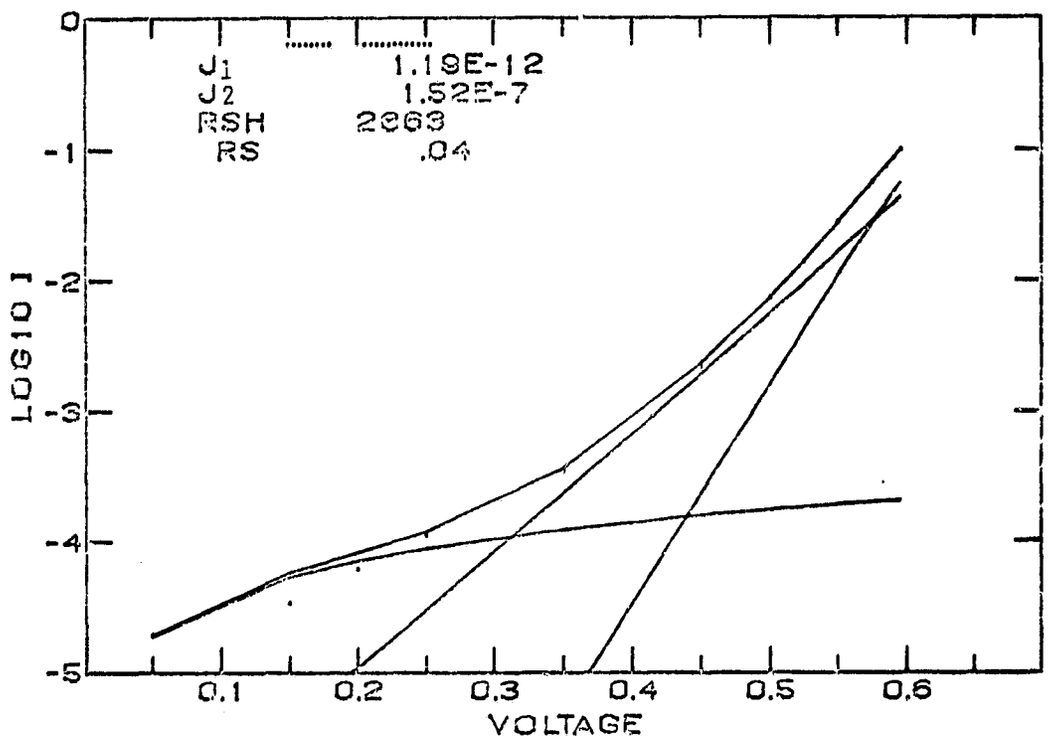


Figure 3-11. Dark IV Curve for a 1250 Ω-cm $n^+pp^+$ Cell Dots are Experimental Data

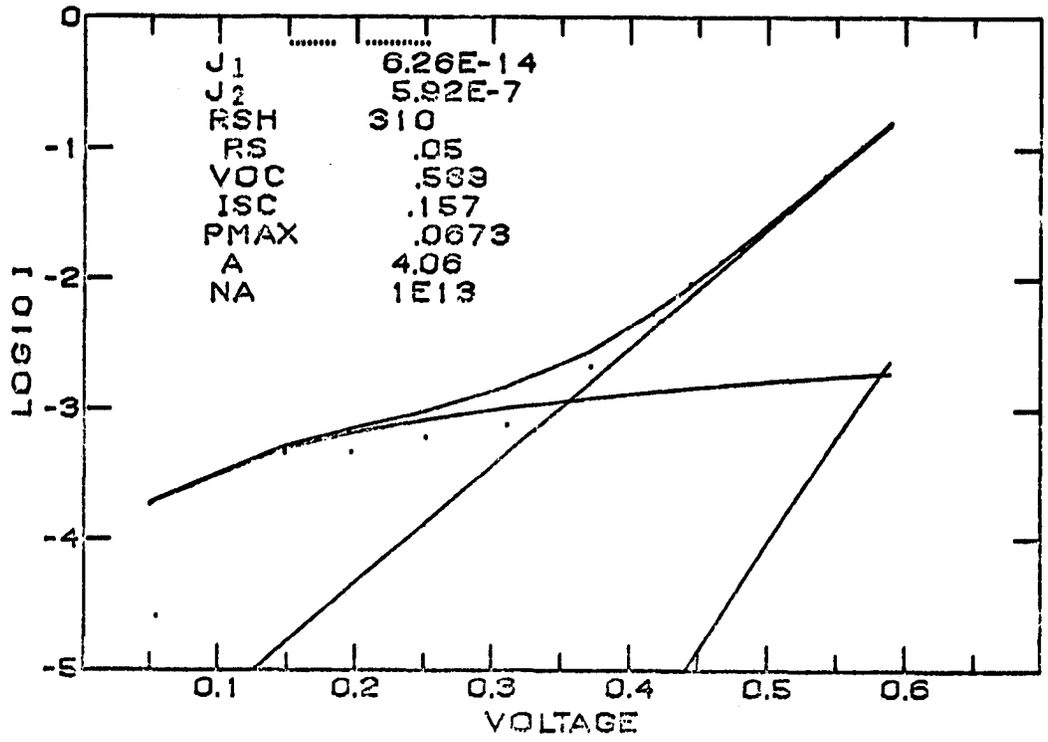


Figure 3-12. Illuminated IV Curve (Minus $I_{sc}$) for the Cell in Figure 3-11. Dots are Experimental Data

data indicate the transition from extrinsic (unilluminated) to intrinsic (when illuminated) operation. The differences between this cell and the previous one are expected since a greater portion of the bulk of the 1250 Ω-cm cell is in the intrinsic regime.

Cells with grid contacts on both surfaces were analyzed to better understand the differences between front and back illuminated (Figure 3-5) I-V characteristics. The results, shown in Figures 3-13 and 3-14, indicate that the values of $J_1$ and $J_2$ are nearly independent of which surface is illuminated. However, the effective shunt resistance determined for front illumination is nearly an order of magnitude lower than that for back-illumination. Three of the possible causes for this difference are described. 1) The shunt resistance is due to leakage across the $n^+$-p junction and is dependent on illumination level. This would explain the differences in shunt resistance for a cell illuminated on the front and back surfaces and the differences between illuminated and unilluminated I-V characteristics. 2) The slope in the I-V curve of a front illuminated cell (Figure 3-5), which the computer analysis attributes to shunt leakage, could result from the negative injection level effects described in the previous section. Since this cell has a lower computed value for shunt resistance and exhibits the negative injection level effect, it is felt that both hypotheses may be contributing in

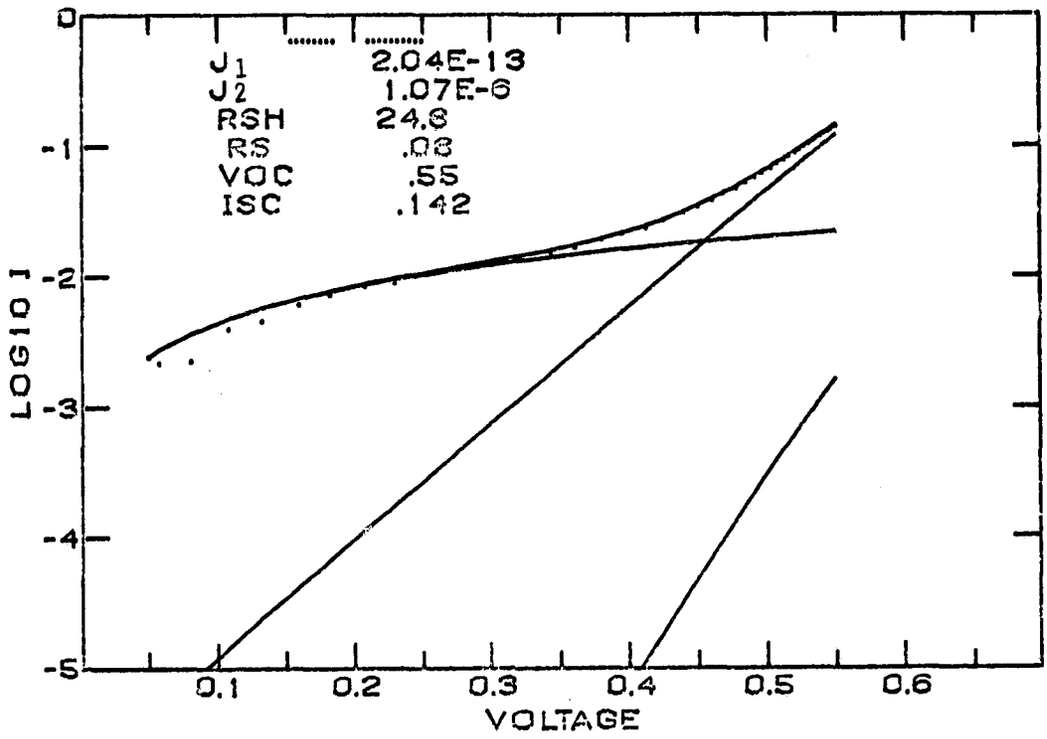


Figure 3-13. IV Analysis of a Front Illuminated 1250 Ω-cm, 250 μm, $n^+pp^+$ Cell. Dots are Experimental Data

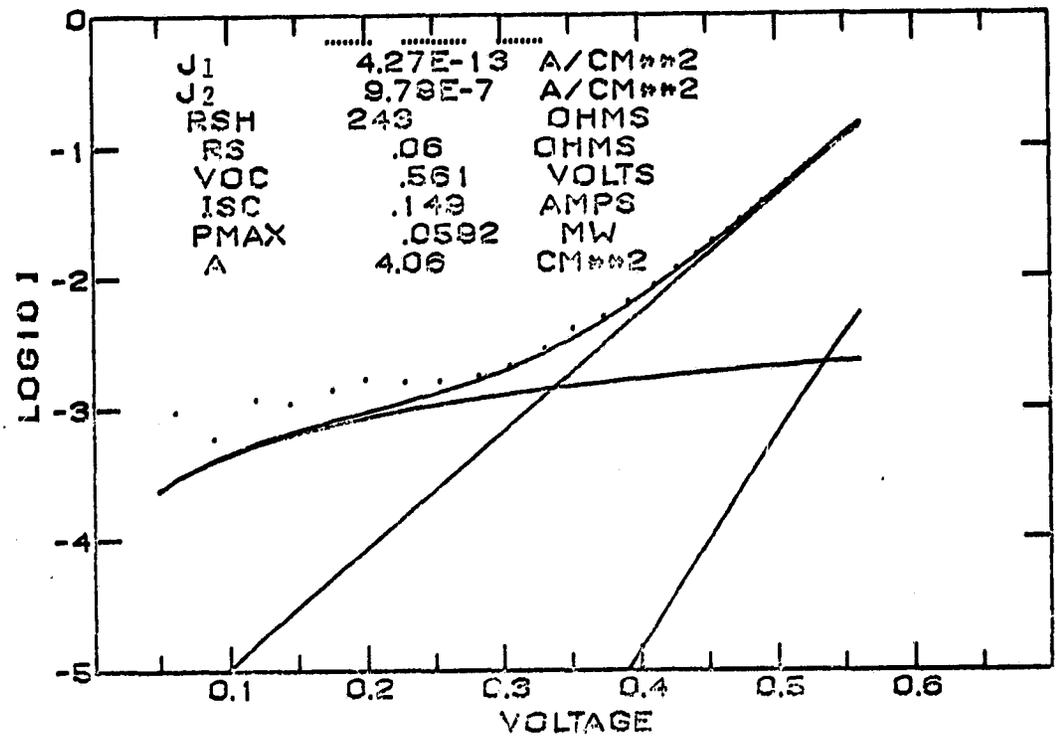


Figure 3-14. IV Analysis of the Cell in Figure 3-13 Under Illumination From the p$^{+}$ Side. Dots are Experimental Data

this case. 3) A Dember potential [13] is developed when cells are illuminated with non-uniformly absorbed light. When illumination is on the $n^+$ side of the cell the Dember potential, as mentioned earlier, is in a direction opposite to that of the junction voltage. As short circuit current conditions are approached, a greater portion of the cell bulk is reverse biased and the slope of the I-V curve is greater than in the case of illumination on the $p^+$ side. The Dember potential has not been included in the I-V analysis program and, therefore, appears as a reduced shunt resistance.

Analysis of a 100 μm, 1250 Ω-cm cell (Figure 3-15) indicates a reduction of the n = 2 component as predicted by Equation 8. However, the open circuit voltage did not increase as much as predicted since the n = 1 term increased unexpectedly. This increase is not due to a return to extrinsic operation, as might be thought from the previous argument, but is caused by an increase in the recombination of carriers in one diffused region that are thermally generated in the other diffused region. This effect has been referred to as a high injection leakage current by Fang and Hauser [14] and their expression for it is

$$J_L = q\, S_o \left(\frac{D_n}{L_n}\right)\left[\frac{N^2(x_{HL})}{N_A}\right] \qquad (10)$$

for $N^2(x_{HL}) >> N_A$. In Equation 10, $N(x_{HL})$ is the carrier concentration adjacent the high-low junction and $S_o$ is a normalized

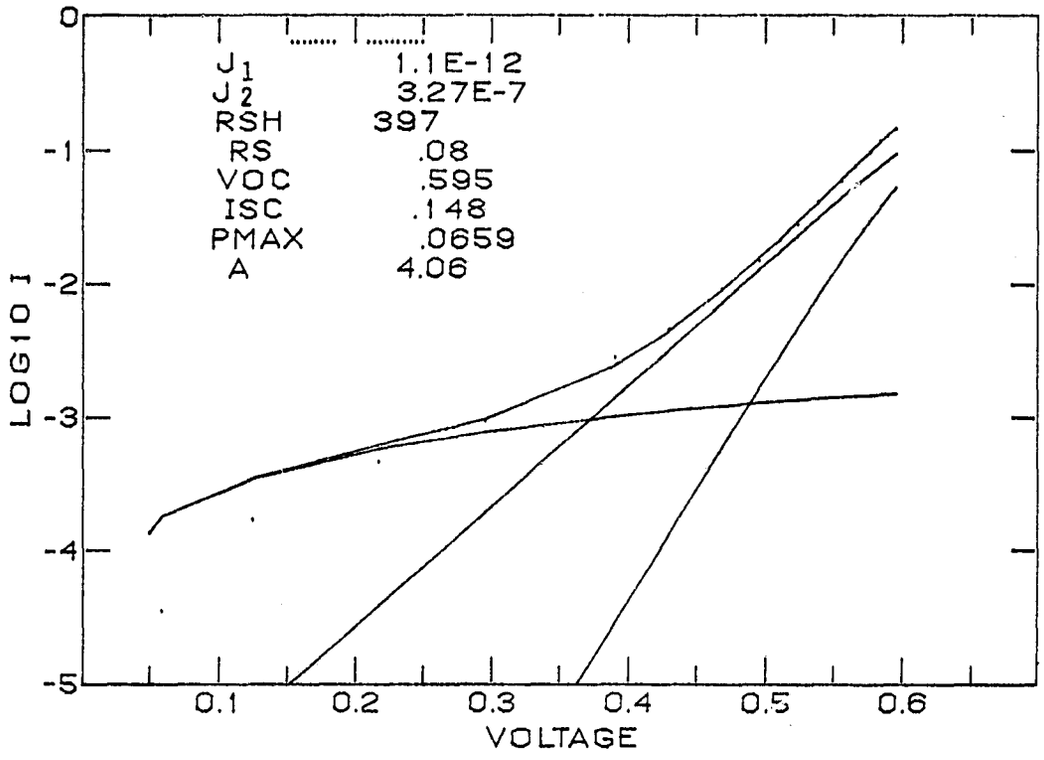


Figure 3-15. IV Analysis of a Front Illuminated 1250 Ω-cm, 100 μm $n^+pp^+$ Cell. Dots are Experimental Data

surface recombination velocity obtained by multiplying the S of Equation 6 by $L_n/D_n$. If, in Equation 6, $S_n >> D_n+/L_n+$, $J_L$ becomes

$$J_L = q\left(\frac{D_n+}{L_n+}\right)\left[\frac{N^2(x_{HL})}{N_A+}\right] \coth \frac{W+}{L_n+} \qquad (11a)$$

or

$$J_L = q\left(\frac{D_n+}{W+}\right)\left[\frac{N^2(x_{HL})}{N_A+}\right] \qquad (11b)$$

as W+ becomes much less than $L_n+$.

Assuming the following values;

$D_n+ = 2.5\ cm^2/sec$

$W+ = 0.2\ \mu m$

$N_A+ = 10^{19}\ cm^{-3}$

$N(x_{HL}) \leqq N(x_{n+p}) = N_i \exp\left[\frac{qV}{2kT}\right]$

the computed value for $J_L$(at V = 0) is $2.8 \times 10^{-13}$ A/cm$^2$ compared to the measured value of $1.1 \times 10^{-12}$ A/cm$^2$ for the 100 μm thick cell. The reasonably good agreement between these values of $J_L$ [considering the uncertainty in $N(x_{HL})$ and $N_A+$] supports the theoretical model and allows extension of it to 250 μm thick cells. In this case $N(x_{HL})$ should be about 45 percent that of the 100 μm thick cell [14] and the predicted value of $J_L$ is $5.6 \times 10^{-13}$ A/cm$^2$ and is in very good agreement with the data shown in Figure 3-13. The difference between the values of $J_1$ of

Figure 3-13 and Figure 3-14 is, now, easily explained since $N(x_{HL})$ is greater for $p^+$ illumination than for $n^+$ illumination. The influence of the carrier concentration on $S_o$ and $J_L$ could contribute to, or account for, the reduction of measured diffusion length with increased injection level (Section 3.4).

## 4. LIMITATIONS

It has been shown in previous sections that, in order to achieve a high efficiency n-i-p cell, certain limitations must be overcome. These are: (1) reduction of bulk diffusion length with illumination, (2) high-low junction leakage current, (3) Dember potential, and (4) lack of high injection conditions throughout the cell bulk. In addition, a limitation, not previously discussed, is the bias caused by the potential drop across the internal resistance of the bulk.

Although the low level quantum efficiency measurements indicated a diffusion length of greater than 2350 μm in 1250 Ω-cm cells, the diffusion lengths occurring under AM0 conditions could be about a factor of five less, or ~470 μm. Since the reduction of diffusion length did not appear to be the same in all of the high resistivity cells, process dependent defects may be the cause. Applying gettering techniques could result in longer diffusion lengths under AM0 conditions.

It was shown in Equation 10 that the high-low junction leakage current is proportional to the square of the carrier concentration at that junction. Reduction of cell thickness would, therefore, seem counter productive since this would result in a higher carrier concentration. It appears that the ideal situation is one in which the carrier concentration is high enough to achieve

intrinsic conditions throughout the bulk of the cell but not so high that this leakage current becomes a serious detriment. There are two other factors ($W^+$ and $N_A+$) that can be optimized to reduce this leakage current. Such a reduction could be accomplished by a deeper, higher doping in the $p^+$ layer.

It was mentioned in Section 3-5 that a Dember potential could account for the apparent low value of shunt resistance seen when cells are illuminated on the $n^+$ side. In this situation the Dember potential is in the opposite direction of the junction voltage and results in a forward bias across the junction when the terminal voltage is zero (i.e. short circuit current condition). This results in a higher slope of the I-V curve at zero terminal voltage and the magnitude of this slope depends upon the magnitude of the Dember potential. It has been shown [13] that the Dember potential between two points 1 and 2 can be written as

$$V_D = \frac{kT}{q}\left(\frac{\mu_n - \mu_p}{\mu_n + \mu_p}\right) \ln \frac{\sigma_2}{\sigma_1} \qquad (12)$$

where $\mu$ is the mobility, $\sigma = q(\mu_n n + \mu_p p)$, and n and p are the electron and hole concentrations, respectively. From this equation, it can be seen that the magnitude of $V_D$ depends on the mobility difference and, more importantly on the ratio of the conductivities. This means that if a high resistivity cell is not uniformly in a high injection mode [15] a large difference in conductivities could exist between the junctions resulting in a

large Dember potential. The Dember potential can be lowered by reducing the cell thickness for cells limited either by leakage current or by bulk dark current [16]. A back surface reflector should reduce the Dember potential since the carrier concentration at the back surface should increase over the case of no reflector.

One limitation incurred by a lack of uniform high injection conditions was mentioned with respect to the Dember potential. Another limitation occurs due to a carrier lifetime (or diffusion length) dependence on excess carrier density. The results of this study and of others have shown that such a dependence may exist. In fact, the results in reference [12] show that the carrier lifetime exhibits a maximum as a function of carrier density. Depending upon which side of the maximum the cell is operating under AM0 illumination, the lifetime may increase or decrease with increasing illumination intensity. In the case of non-uniform injection, then, one may obtain a wide variation in diffusion length within the bulk. Such structures could display significantly altered current collection and voltage dependence upon L. The I-V curve analysis is much more complicated in such a situation. It is essential to use thi. cells to correct this condition.

The last limitation of those mentioned is the potential drop across the internal resistance. This resistance, in a

1250 Ω-cm cell that is 250 μm thick, is about 31 Ω-cm$^2$ under equilibrium conditions. If a uniform concentration of electrons and holes of $10^{14}$ cm$^{-3}$ density is injected, (either by long wavelength illumination or a forward bias of ~0.45 V [17], the internal resistance drops to about 0.8 Ω-cm$^2$. This is not too serious a limit for a 4 cm$^2$ cell but this value represents a lower limit for the case of non-uniform injection. Not only does this internal resistance reduce the I-V fill factor but, in the case of non-uniform injection, it can alter the cell bias in a manner similar to that described for the Dember potential. Long carrier lifetime and thin cells are required to keep this limitation to a minimum.

## 5. CONCLUSIONS AND PROSPECTS FOR n-i-p CELLS

The goal of this feasibility study was to demonstrate that a solar cell can be fabricated from high resistivity material without sacrificing open circuit voltage. In order to achieve this goal the cell must have a good $p^+$ back contact and maintain high carrier lifetime. A $p^+$ layer formed by diffusion of boron from a spin-on source has resulted in an effective surface recombination velocity of about 1 cm/sec under low injection conditions and less than 100 cm/sec under AM0 conditions. Cells with this $p^+$ layer have exhibited open circuit voltages that increase with decreasing cell thickness and that approach 600 mV.

A secondary objective of this study was to achieve a good $p^+$ layer, while maintaining an optical quality good enough for application of a back surface reflector. This achievement was demonstrated by high (nearly the theorical maximum value of 85 percent) cell reflectivity at 1.5 μm with an aluminum reflector applied over the boron $p^+$ layer.

Limitations (and possible means of alleviating them) to achieving even better cell performance than obtained in this study have been described in Section 4 of this report. Since this study was concerned with the bulk lifetime and back surface effects, a reliable, although not optimum, n-type diffused layer was employed throughout. Optimization studies of both n and $p^+$ layers will

lead to improved cell output and should be made for high resistivity material. In addition, radiation damage coefficients and carrier lifetimes should be determined on high resistivity material as a function of illumination conditions and bulk resistivity.

When the limitations, as presented, are eliminated or alleviated; an open circuit voltage of ~650 mV should be achievable under AM0 conditions. This will come only at the price of somewhat reduced short circuit current due to the necessary reduction in cell thickness. However, with means already available, a short circuit current of about 43 $mA/cm^2$ should be attainable in a 50 μm thick cell by using textured surfaces and back surface reflectors. Even if the fill factor cannot be improved beyond 0.76, these values translate to an output of about 21 $mW/cm^2$, or an efficiency of about 15.6 percent for a cell that is potentially radiation tolerant.

# 6. NEW TECHNOLOGY

No new technology was developed in this study.

## 7. REFERENCES


[1] J. F. Allison, R. A. Arndt, and A. Meulenberg, COMSAT Technical Rev. 5, 211 (1975).

[2] J. Lindmayer and J. F. Allison, Proc. of the 9th Photovoltaic Specialists Conference, Silver Spring, Md. May 1972; pp. 53-84 COMSAT Technical Review, 3, 1 (1973).

[3] J. G. Haynos, J. F. Allison, R. A. Arndt and A. Meulenberg, International Conference on Photovoltaic Power Generation, Hamburg, Germany, 1974, pp. 487-500.

[4] See, for example, J. Mandelkorn and J. H. Lamneck, Proc. of the 9th Photovoltaic Specialists Conference, Silver Spring, Md. May 1972, pp. 66-71.

[5] See, for example, H. Y. Tada and J. R. Carter, "The Solar Cell Radiation Handbook," J. P. L. Publication 77-56, November 1977.

[6] See, for example, J. P. McKelvey, "Solid State and Semiconductor Physics," Harper and Row, N. Y., 1966, Ch. 13.

[7] J. B. Gunn, Jl. of Electronics and Control, 4, 17 (1958).

[8] M. P. Godlewski, C. R. Baraona, and H. W. Brandhorst, Proc. of the 10th Photovoltaic Specialists Conference, Palo Alto, CA. November 1973, pp. 40-49.

[9] R. N. Hall, Proc. IRE, 40, 1512 (1952).

[10] N. M. Bordina et. al., Applied Solar Energy (Geliotechnika from the Russian) 14, 1 (1978).

[11] A. G. Sabnis, Solid State Electronics, 21, 581 (1978).

[12] J. R. Srour and O. L. Curtis, Jr., J. Appl. Phys. 43, 1779 (1972).

[13] See, for example, S. M. Ryvkin, "Photoelectric Effects in Semiconductors," Consultants Bureau, N.Y., 1964, pg. 63.

[14] R. C. Y. Fang and J. R. Hauser, Annual Report on NASA Grant NGR 34-002-195, "A Theoretical Analysis of the Current-Voltage Characteristics of Solar Cells," Sept. 1977.

[15] Yu. M. Altayskiy and V. S. Kiselev, Radio Engineering and Electronic Physics 20, 69 (1975). Trans. from the Russian.

[16] A. M. Vasil'yev, Radio Engr. and Electronic Physics, 13, 83 (1968) Trans. from the Russian.

[17] P. M. Dunbar and J. R. Hauser, Annual Report on NASA Grant NGR 34-002-195, Solar Cells," Aug. 1975.

## APPENDIX A. TYPICAL 50 μm n-i-p CELL FABRICATION PROCESS

1. Inspect, measure and clean incoming material.
2. Grow mask oxide for thinning 1050°C-4 hrs. 95°C $H_2O$ vapor (8500 Å).
3. Pattern and etch oxide.
4. Thinning etch-10 percent KOH, 85°C, 140 min.
5. Spin-on Borosilica 0317 and diffuse 950°C-30 min.
6. Post diffusion clean-up.
7. Spin-on N-250 and diffuse 850°C-15 min.
8. Post diffusion clean-up.
9. Evaporate Ta-280Å.
10. Pattern grids.
11. Evaporate Cr-Au and lift-off excess metal.
12. Evaporate Cr-Au back contact.
13. Ag plate ≅ 5 μm.
14. Oxidize Ta 525°C-5 min.
15. Saw.
16. Test.

## APPENDIX B. CURRENT-VOLTAGE EQUATIONS FOR NON-UNIFORM ILLUMINATION OF HIGH RESISTIVITY CELLS

The situation described by the following equations is shown in the figure below:

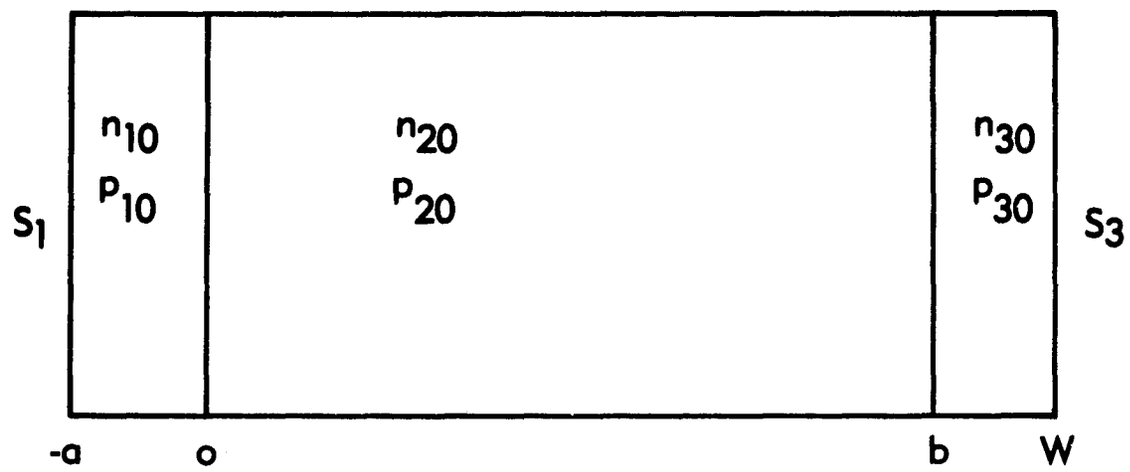


The $n^+$-p junction is at the origin and the p-$p^+$ junction is at b. Region 1 is $n^+$, region 2 is p, and region 3 is $p^+$ type material. For each region and wavelength, the excess carrier density ($\delta n$) is represented by an equation of the form

$$\delta n = A \cosh \frac{X}{L} + B \sinh \frac{X}{L} + g\tau e^{-\alpha(x + a)} \qquad \text{(B-1)}$$

where the constants (A and B) are evaluated in terms of the boundary conditions. In equation B-1, L is the diffusion length, $\tau$ is the carrier lifetime, and $\alpha$ is the optical absorption coefficient. The generation term, g, is

$$g = \frac{\alpha F}{1-\alpha^2 L^2} \qquad \text{(B-2)}$$

where F is the photon fluence entering the solar cell.

If it is assumed that the currents across each junction are purely diffusive in nature one can then write the expressions for the currents densities and these are:

$$J_I = \frac{J_o + J_o' \exp[-q(\phi_o - V_o)/kT]}{1 - \exp[-2q(\phi_o - V_o)/kT]} \left[\exp\left(\frac{qV_o}{kT}\right) - 1\right]$$

$$- \frac{J_o'' + J_o'''\exp[-q(\phi_b - V_b)/kT]}{1 - \exp[-2q(\phi_b - V_b)/kT]} \left[\exp\left(\frac{qV_b}{kT}\right) - 1\right] - J_{\ell o} \qquad \text{(B-3)}$$

$$J_{II} = \frac{J_b + J_b' \exp[-q(\phi_o - V_o)/kT]}{1 - \exp[-2q(\phi_o - V_o)/kT}} \left[\exp\left(\frac{qV_o}{kT}\right) - 1\right]$$

$$- \frac{J_b'' + J_b''' \exp[-q(\phi_b - V_b)/kT]}{1 - \exp[-2q(\phi_b - V_b)/kT]} \left[\exp\left(\frac{qV_b}{kT}\right) - 1\right] - J_{\ell b} \qquad \text{(B-4)}$$

In Equations B-3 and B-4 the $\phi$'s are the equilibrium potentials, the V's are developed potentials, and k, T, and q have the usual meaning. The J's are material and structure dependent and are:

$$J_o = \frac{qD_1}{L_1} \gamma_1 p_{10} + \frac{qD_2}{L_2} n_{20} \coth\left(\frac{b}{L_2}\right)$$

$$J_o' = \frac{qD_1}{L_1} \gamma_1 n_{10} + \frac{qD_2}{L_2} p_{10} \coth\left(\frac{b}{L_2}\right)$$

$$J_o'' = \frac{qD_2}{L_2} p_{20} \operatorname{csch}\left(\frac{b}{L_2}\right)$$

$$J_o''' = \frac{qD_2}{L_2} n_{30} \operatorname{csch}\left(\frac{b}{L_2}\right)$$

$$J_b = \frac{qD_2}{L_2} n_{20} n_{20} \operatorname{csch}\left(\frac{b}{L_2}\right)$$

$$J_b' = \frac{qD_2}{L_2} p_{10} \operatorname{csch}\left(\frac{b}{L_2}\right)$$

$$J_b'' = \frac{qD_2}{L_2} p_{20} \coth\left(\frac{b}{L_2}\right) + \frac{qD_3}{L_3} n_{30} \gamma_3$$

$$J_b''' = \frac{qD_2}{L_2} n_{30} \coth\left(\frac{b}{L_2}\right) + \frac{qD_3}{L_3} p_{20} \gamma_3.$$

The terms D, L, n, and p have their usual meaning and the subscripts 10, 20, 30 refer to equilibrium concentrations in the respective regions.

The generated current densities for illumination on the $n^+$ side, are:

$$J_{\ell o} = \frac{qD_1 g_1 \tau_1}{L_1} (\gamma_1 e^{-a\alpha} - \theta_1) + \frac{qD_2 g_2 \tau_2}{L_2} e^{-a\alpha}$$

$$\left[\coth\left(\frac{b}{L_2}\right) - e^{-\alpha b} \operatorname{csch}\left(\frac{b}{L_2}\right)\right] \qquad \text{(B-5)}$$

$$+ q\alpha e^{-a\alpha} (D_1 g_1 \tau_1 - D_2 g_2 \tau_2)$$

and

$$J_{\ell b} = \frac{qD_2 g_2 \tau_2}{L_2} e^{-a\alpha} \left[\operatorname{csch}\left(\frac{b}{L_2}\right) - e^{-\alpha b} \coth\left(\frac{b}{L_2}\right)\right]$$

$$- \frac{qD_3 g_3 \tau_3}{L_3} e^{-a\alpha} [\gamma_3 e^{-\alpha b} - \theta_3 e^{-\alpha W}] \qquad \text{(B-6)}$$

$$- \alpha q e^{-\alpha(a+b)} (D_2 g_2 \tau_2 - D_3 g_3 \tau_3)$$

In the above expresions, the $\gamma$ and $\phi$ terms are:

$$\gamma_1 = \frac{S_1 \cosh\left(\frac{a}{L_1}\right) + \frac{D_1}{L_1} \sinh\left(\frac{a}{L_1}\right)}{S_1 \sinh\left(\frac{a}{L_1}\right) + \frac{D_1}{L_1} \cosh\left(\frac{a}{L_1}\right)} \qquad \theta_1 \frac{S_1 + \alpha D_1}{S_1 \sinh\left(\frac{a}{L_1}\right) + \frac{D_1}{L_1} \cosh\left(\frac{a}{L_1}\right)}$$

$$\gamma_3 = \frac{S_3 \cosh\left(\frac{W-b}{L_3}\right) + \frac{D_3}{L_3} \sinh\left(\frac{W-b}{L_3}\right)}{S_3 \sinh\left(\frac{W-b}{L_3}\right) + \frac{D_3}{L_3} \cosh\left(\frac{W-b}{L_3}\right)} \qquad \theta_3 = \frac{S_3 - \alpha D_3}{S_3 \sinh\left(\frac{W-b}{L_3}\right) + \frac{D_3}{L_3} \cosh\left(\frac{W-b}{L_3}\right)}$$

where $S_1$ and $S_3$ are the surface recombination velocities.

When the cell is illuminated on the $p^+$ side, all of the script $J_o$ and $J_b$ terms and the $\gamma$ terms remain the same as for illumination on the $n^+$ side. In this case, however,

$$\theta_1 \rightarrow \theta_1' = \frac{S_1 - \alpha D_1}{S_1 \sinh\left(\frac{a}{L_1}\right) + \frac{D_1}{L_1}\cosh\left(\frac{a}{L_1}\right)}$$

$$\theta_3 \rightarrow \theta_3' = \frac{S_3 + \alpha D_3}{S_3 \sinh\left(\frac{W-b}{L_3}\right) + \frac{D_3}{L_3}\cosh\left(\frac{W-b}{L_3}\right)}$$

and

$$J_{\ell o} \rightarrow J_{\ell o}' = \frac{qD_1 g_1 \tau_1}{L_1}\left[\gamma_1 e^{-\alpha W} - \theta_1' e^{-\alpha(a+W)}\right]$$

$$+ \frac{qD_2 g_2 \tau_2}{L_2} e^{-\alpha W}\coth\left(\frac{b}{L_2}\right) - e^{-\alpha(W-b)}\operatorname{csch}\left(\frac{b}{L_2}\right)$$

$$-\alpha q e^{-\alpha W}(D_1 g_1 \tau_1 - D_2 g_2 \tau_2)$$

and

$$J_{\ell b} \rightarrow J_{\ell b}' = \frac{qD_2 g_2 \tau_2}{L_2}\left[e^{-\alpha W}\operatorname{csch}\left(\frac{b}{L_2}\right) - e^{-\alpha(W-b)}\coth\left(\frac{b}{L_2}\right)\right]$$

$$- \frac{qD_3 g_3 \tau_3}{L_3}\left[\gamma_3 e^{-\alpha(W-b)} - \theta_3'\right]$$

$$+ \alpha q e^{-\alpha(W-b)}(D_2 g_2 \tau_2 - D_3 g_3 \tau_3)$$

These equations were solved numerically for open circuit voltage by setting the $J_I$ and $J_{II}$ equal to zero. The results are shown in Table B-1 for a 1250 Ω-cm, 250 μm thick cell.

Table B-1. Open Circuit Voltage for Front and Rear Illumination

| Illum | $V_{oc}$(mV) Exp | Theory |
|---|---|---|
| Front | | |
| AM0 | 556 | 550 |
| Back | | |
| AM0 | 566 | 561 |
| 3000 K | | |
| Front | 530 | 580 |
| 3000 K | | |
| Back | 590 | 641 |

The differences in $V_{oc}$ between front and back illumination are very nearly equal whether determined experimentally or theoretically. Actual values are not close in the case of 3000°K illumination. However, this is not too surprising since the values chosen for parameters such as carrier lifetime and surface recombination velocity may not truly represent those actually occurring in practice.

## APPENDIX C. PVSC PAPER

The attached paper was prepared and presented at the 14th Photovoltaic Specialists Conference January 7-10, 1980, San Diego, California.

# THIN n-i-p SILICON SOLAR CELL*

A. Meulenberg, Jr., J. F. Allison, and R. A. Arndt

COMSAT Laboratories
Clarksburg, MD 20734

## INTRODUCTION

One major concern in the application of solar cells for use in space is their susceptibility to degradation from the radiation environment. The reduction in cell output is attributed to loss primarily in current caused by a reduction of minority carrier diffusion length (L) in the bulk of the cell. The standard expression for the reduction is

$$\frac{1}{L^2} = \frac{1}{L_o^2} + K\phi \qquad (1)$$

where $L_o$ and L are the diffusion lengths before and after irradiation, respectively; K is a constant of proportionality; and $\phi$ is the radiation fluence. When the diffusion length approaches and becomes less than the thickness of the bulk region, significant current loss results and, of course, the power output drops. It is known that the reduction of diffusion length due to radiation can be alleviated by increasing the resistivity of the bulk material, since the constant K decreases as resistivity increases. However, as the base resistivity increases, the cell voltage decreases resulting in reduced power output. The concept presented below combines high cell output with low diffusion length damage coefficients.

## THEORY

The simplified diode equation commonly applied to solar cells is

$$J = J_o \left[\exp \frac{qV}{AkT} - 1\right] - J_\ell \qquad (2)$$

where J, $J_o$, and $J_\ell$ are the cell current, the cell saturation current, and the photogenerated current, respectively; V is the cell voltage; and A is the diode quality factor. Under open circuit conditions, J is zero and

$$V_{oc} = \frac{AkT}{q} \ln \frac{J_\ell}{J_o} \quad . \qquad (3)$$

In a $n^+$-p junction solar cell, $J_o$ consists primarily of contributions from the bulk of the cell and the $n^+$ region (neglecting recombination in the space charge layers). Because the $n^+$ layer is very heavily doped, its contribution is usually very small with respect to the contribution from the p region and

$$J_o = \frac{qn_o D_n}{L_n}\left[\frac{S\cosh(W/L_n) + D_n/L_n \sinh(W/L_n)}{D_n/L_n \cosh(W/L_n) + S\sinh(W/L_n)}\right] \qquad (4)$$

where $n_o$, $D_n$, and $L_n$ are the equilibrium carrier density, diffusion constant, and diffusion length of electrons in the p region of length W, respectively, and S is the surface recombination velocity at the back surface of the cell. If $S \ll D_n/L_n$, equation (4) can be written

$$J_o = \frac{qn_i^2}{N_A}\frac{D_i}{L_n} \times \tanh\frac{W}{L_n} \quad . \qquad (5)$$

The expression $n_o p_o = n_i^2 = n_o N_A$ and the assumption that all of the acceptors ($N_A$) are ionized have been used. Equation (5) reduces to

$$J_o = \frac{qn_i^2}{N_A}\frac{D_n W}{L_n^2} = \frac{qn_i^2}{N_A}\frac{W}{\tau} \qquad (6)$$

if $W \ll L_n$. As the bulk material changes from p type to intrinsic, $J_o$ approaches

$$J_o = \frac{qn_i W}{\tau} \quad . \qquad (7)$$

*This paper is based upon work performed at COMSAT Laboratories under the sponsorship of the Communications Satellite Corporation and supported in part by NASA-LeRC under Contract NAS3-21280.

Using equation (7) and the practically realizable goals of $J_\ell$ = 40 mA/cm$^2$ (under AMO illumination), W = 50 μm, and τ = 200 μs, an open circuit voltage of 693 mV is calculated. The diode quality factor has a value of two [which contributes to the high value of $V_{OC}$, equation (3)] instead of unity which is usually found in more heavily doped bulk regions. This higher diode factor will result in a lower fill factor; however, if a value of 0.75 is maintained, the output power and efficiency will be ≈21 mW/cm$^2$ and 15.4 percent, respectively.

Radiation damage effects will not become significant in the $J_\ell$ term of equation (2) until very high exposures are experienced, and the carrier diffusion length is reduced to less than three times the cell thickness. However, any reduction in lifetime will affect the $J_o$ term [equation (7)] and reduce the open circuit voltage. Nevertheless, it is expected that the damage rates of τ or L will be much lower than in extrinsic material. Since the Fermi level will be at mid-band, the radiation induced defects are more likely to be in neutral charge status and, therefore, result in lower capture cross sections for recombination.

Further background for n-i-p solar cells can be found in power transistor work, concentrator solar cell studies, and computer solutions (1). A recent paper (2) provides a theoretical description and presents similar experimental results.

## EXPERIMENTS AND RESULTS

Development of the n-i-p cell has been approached as an extension of the relatively well understood theory of 1-10 Ω-cm cells to increasingly higher resistivity material. The $p^+$ backs were applied by diffusion from a spin-on boron diffusion source. The higher $p^+$ doping of the boron in this source should more than compensate for the loss of possible gettering by an aluminum melt.

The AMO illuminated characteristic of a 1250 Ω-cm, 100 μm thick n-i-p cell, covered with 150 μm thick CMS is illustrated in Figure 1. This 4 cm$^2$ cell produces 158.3 mA at short circuit, 591.5 mV at open circuit, and a peak power of 69 mW with 0.16 Ω series resistance producing a fill factor of 73.4 percent. Also shown is the AMO illuminated curve of an identically processed 250 μm thick cell. The poor fill factor (65.7 percent) appears due both to additional series resistance (0.54 Ω) and shunt leakage at the back i-$p^+$ junction equivalent to 25 Ω. Note the increased $V_{OC}$, as expected from equation (7).

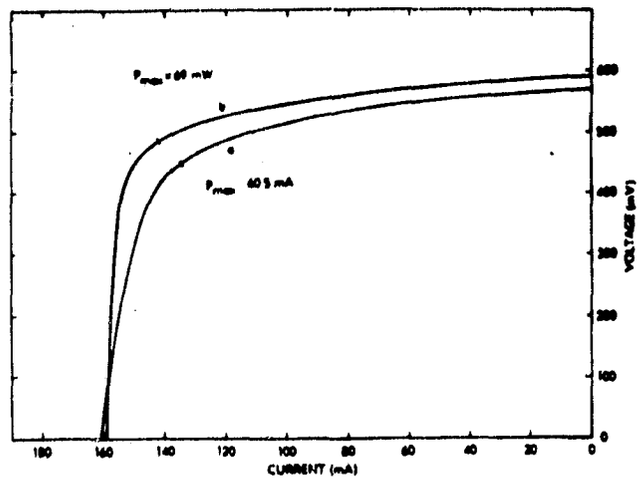


Figure 1. I-V Characteristic of 250 μm Thick (a) and 100 μm Thick (b) 1250 Ω-cm, $n^+$-p-$p^+$ Solar Cells Under AMO Illumination

Additional 250 μm thick cells have been fabricated in both 83 and 1250 Ω-cm silicon with grid contact fingers and A-R coatings on both sides. The I-V characteristic of an 83 Ω-cm cell with AMO illumination incident on the $n^+$ and the $p^+$ surfaces is shown in Figure 2. An effect often observed in thick, high resistivity cells is a higher fill factor when the cell is illuminated from the $p^+$ rather than from the $n^+$ side. This effect and the difference in $V_{OC}$, which varies strongly with the spectral distribution of the illuminating source, appears to be due to the Dember potential and the spatial variation of the Fermi level relative to the band edge in the bulk. Similar measurements were obtained from the 1250 Ω-cm cell; the resulting I-V curves are shown in Figure 3.

The low-level spectral response of these cells was measured with the $n^+$ and $p^+$ sides illuminated separately, and the internal quantum efficiency (QE) was then calculated. These data are shown in Figures 4 and 5 for the 83 and 1250 Ω-cm cells, respectively. The QE of the 83 Ω-cm cell with $p^+$ side illumination is approximately one-half of the QE with $n^+$ side illumination over the wavelength range of 450 to 850 nm. At wavelengths below 400 nm, both the $n^+$ and $p^+$ side QE indicate the presence of some "dead layer" at both surfaces. The nearly equal QE at wavelengths >1000 nm is expected, since the carrier profile generated in the bulk material is insensitive to which side is illuminated. The diffusion length calculated from these low-level data is between 250 and 400 μm, depending upon the value assumed for the surface recombination

velocities. An increase in L with injection level was observed which could account for the apparent discrepancy between the data in Figures 2 and 4. The QE determined for the 1250 Ω-cm cell (Figure 5) indicates nearly identical collection with either $n^+$ or $p^+$ side illumination. Again both surfaces exhibit a "dead layer" and excellent long wavelength collection. The low-level diffusion length calculated from the QE exceeds 750 μm.

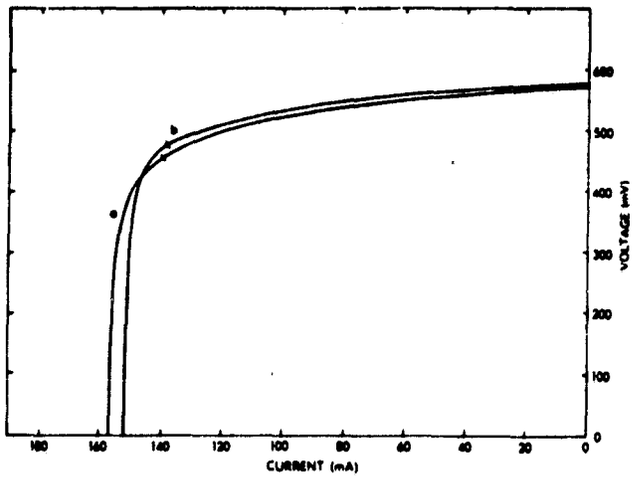


Figure 2. I-V Characteristic of a 250 μm Thick, 83 Ω-cm Solar Cell with AMO Illumination Incident on $n^+$ (a) and $p^+$ (b) Sides

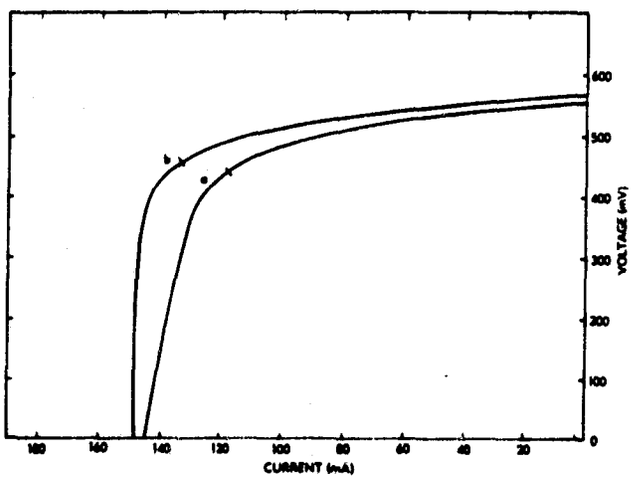


Figure 3. I-V Characteristic of a 250 μm Thick, 1250 Ω-cm Solar Cell with AMO Illumination Incident on the $n^+$ (a) and $p^+$ (b) Sides

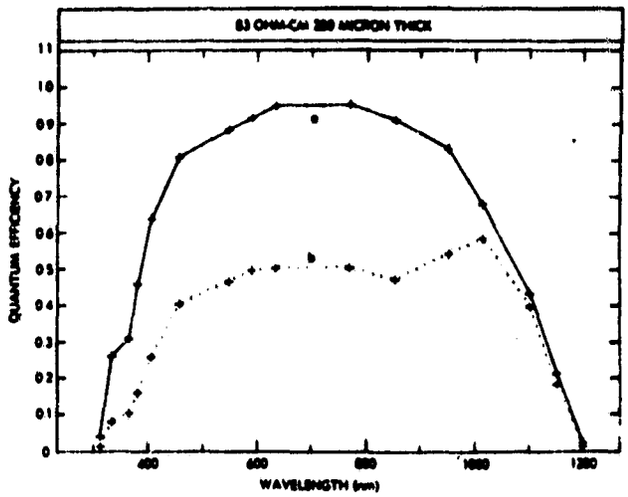


Figure 4. Internal Quantum Efficiency vs Incident Light Wavelength as Measured with Light Incident on the $n^+$ (a) and $p^+$ (b) Sides for a 83 Ω-cm, 250 μm Thick Cell

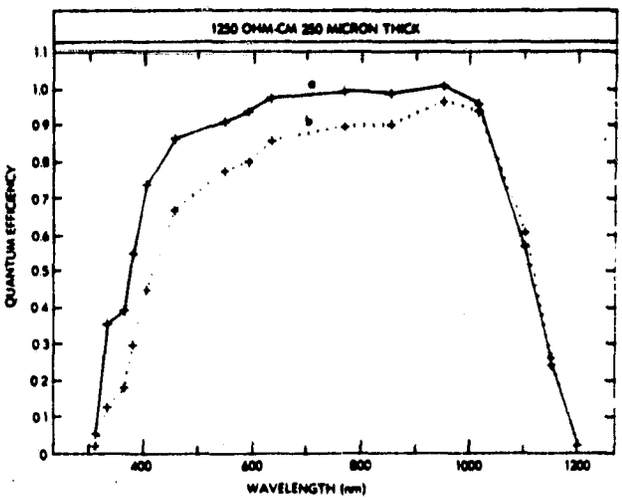


Figure 5. Internal Quantum Efficiency vs Incident Light Wavelength as Measured with Light Incident on the $n^+$ (a) and $p^+$ (b) Sides for 1250 Ω-cm, 250 μm Thick Cells

Spectral response measurements as a function of injection level on the 1250 Ω-cm, 250 μm thick cells revealed a significant reduction of response at all wavelengths as the background illumination approached AMO conditions. This effect was more pronounced with illumination of the $n^+$ side and explains the low values of $I_{sc}$ observed in Figure 3. Similar measurements on lower resistivity cells showed no significant injection level effects.

The results of these experiments indicate that the high resistivity cells do

not behave as expected from the extrapolation of measurements on low resistivity cells. Although a complete model has not been developed, some insight can be gained by noting where conventional models break down as the bulk material approaches intrinsic character.

## MODELS AND ANALYSIS

The diode quality factor, A, can be understood by observing the fraction of the built-in potential which a carrier surmounts between thermal generation and recombination. For example, in low resistivity cells, almost all of the built-in voltage occurs across the p-n junction. In this case, a carrier generated in the p region must surmount the full barrier to recombine in the n layer, but only one-half the barrier to recombine in the center of the junction region. Since the cell voltage, V, does not seriously disturb the potential distribution of the built-in voltage, the carriers in both cases will contribute to the current as exp (qV/kT) and exp (qV/2kT), respectively. In the past, these two components have been combined to produce a single exponential in which the value of A varies between 1 and 2. In the ideal n-i-p cell, the whole bulk i-region is near mid-potential; therefore, the A = 2 term dominates and any A = 1 contribution must be from carriers generated in a diffused region which recombined in the other diffused region. As a first order model, computer fitting of dark or illuminated IV data to

$$J = J_{01} \exp\left(\frac{qV_j}{kT}\right) + J_{02} \exp\left(\frac{qV_j}{2kT}\right) + \frac{V_j}{RSH} - J_\ell \qquad (8)$$

will indicate whether a cell is operating as an intrinsic or extrinsic device.

Analysis of an IV curve from a 1250 Ω-cm cell measured under AMO illumination is shown in Figure 6; the A = 2 component is completely dominant. The same cell measured in the dark shows a dominant A = 1 component (Figure 7). Obviously, the light injected carriers have forced the cell from extrinsic to intrinsic operation. It should be noted in cells where the condition W ≥ L exists the intrinsic region may not extend completely from the $n^+$ to the $p^+$ layer. The influence of this effect is similar but opposite, in sense, to that of the Dember potential which results from the difference in electron and hole mobilities.

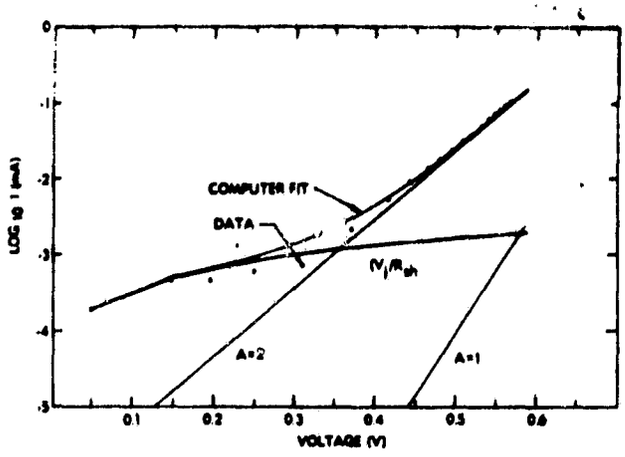


Figure 6. $\text{Log}_{10}$ (I - $I_{sc}$) vs V Plot of a 1250 Ω-cm, 250 μm Thick Solar Cell Under AMO Illumination Showing Actual Data (...), Computer Fit to Equation (8) and Individual A = 1, A = 2, and Shunt Resistance Components

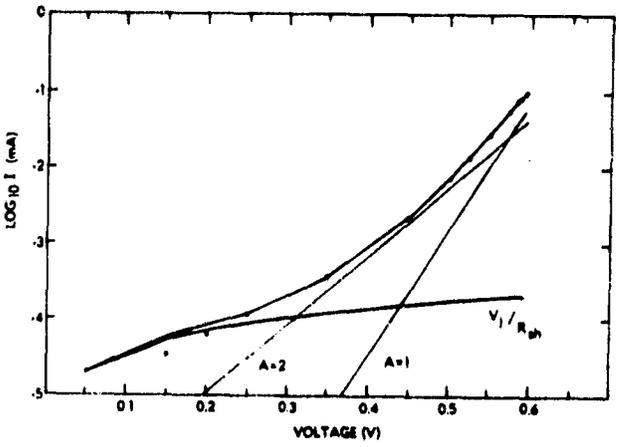


Figure 7. $\text{Log}_{10}$ I vs V Plot of the Cell of Figure 6 with Data Taken Under Nonilluminated Conditions and the Resulting Computer Fit with A = 1, A = 2, and Shunt Resistance Components

Variation of the Fermi level with respect to the band edges through the bulk region (a consequence of nonuniform carrier generation causing the transition from intrinsic to extrinsic material) prevents a specific value of A from being assigned. Carriers generated in the extrinsic region of the bulk surmount more than

one-half the barrier if they recombine in one diffused region (∴ A < 2) and less than one-half the barrier if they recombine in the other (∴ A > 2). When fit to an equation with only A = 1 or A = 2 components, an A value greater than 2 may appear as low shunt resistance and increased series resistance. A further complication arises from the variation of carrier density with current drain from the device. Maximum carrier density is obtained at $V_{oc}$ and minimum carrier density at $I_{sc}$. There is not only a continuum of values for A, but the carrier distribution is a function of illumination (intensity and spectral distribution) and of cell voltage.

## CONCLUSIONS

It has been shown that high resistivity solar cells ($\rho \gtrsim 83$ Ω-cm) act as extrinsic devices under dark conditions and as intrinsic devices under AMO illumination. Resistive losses in a thin n-i-p cell are comparable to those in low resistivity cells. Present voltage limitations appear to be due to generation and recombination in the diffused regions.

A detailed study of the characteristics of high resistivity cells under irradiation to determine if they are more radiation resistant than low resistivity cells will be performed.

## References

1. P. M. Dunbar and J. R. Hauser, "A Theoretical Analysis of the Current-Voltage Characteristics of Solar Cells," Final Report NASA Grant NGR 34-002-195, August 1975.

2. N. M. Bordina et al., "Investigation of the Photoelectric Characteristics of High-Resistivity Silicon Photoconverters," Geliotekhnika, Vol. 14, No. 6, pp. 3-11, 1978, and Applied Solar Energy, Vol. 14, No. 6, 1978.